

## EXPLOSIVE NUCLEOSYNTHESIS IN HYPERNOVAE

TAKAYOSHI NAKAMURA<sup>1</sup>, HIDEYUKI UMEDA<sup>2,8</sup>, KOICHI IWAMOTO<sup>3</sup>, KEN'ICHI NOMOTO<sup>4,8</sup>,  
MASA-AKI HASHIMOTO<sup>5</sup>, W. RAPHAEL HIX<sup>6</sup>, AND FRIEDRICH-KARL THIELEMANN<sup>7</sup>*Accepted for publication in the Astrophysical Journal (13 March 2001)*

## ABSTRACT

We examine the characteristics of nucleosynthesis in 'hypernovae', i.e., supernovae with very large explosion energies ( $\gtrsim 10^{52}$  ergs). We carry out detailed nucleosynthesis calculations for these energetic explosions and compare the yields with those of ordinary core-collapse supernovae. We find that both complete and incomplete Si-burning takes place over more extended, lower density regions, so that the alpha-rich freezeout is enhanced and produces more Ti in comparison with ordinary supernova nucleosynthesis. In addition, oxygen and carbon burning takes place in more extended, lower density regions than in ordinary supernovae. Therefore, the fuel elements O, C, Al are less abundant while a larger amount of Si, S, Ar, and Ca ("Si") are synthesized by oxygen burning; this leads to larger ratios of "Si"/O in the ejecta. Enhancement of the mass ratio between complete and incomplete Si-burning regions in the ejecta may explain the abundance ratios among iron-peak elements in metal-poor stars. Also the enhanced "Si"/O ratio may explain the abundance ratios observed in star burst galaxies. We also discuss other implications of enhanced [Ti/Fe] and [Fe/O] for Galactic chemical evolution and the abundances of low mass black hole binaries.

*Subject headings:* Galaxy: evolution — hypernovae: general — nucleosynthesis — supernovae: individual (SN1998bw) — supernovae: general — stars: abundances

## 1. INTRODUCTION

Massive stars in the range of 8 to  $\sim 150 M_{\odot}$  undergo core-collapse at the end of their evolution and become Type II and Ib/c supernovae unless the entire star collapses into a black hole with no mass ejection (e.g., Arnett 1996). These Type II and Ib/c supernovae (as well as Type Ia supernovae) release large explosion energies and eject explosive nucleosynthesis materials, thus having strong dynamical, thermal, and chemical influences on the evolution of interstellar matter and galaxies. Therefore, the explosion energies of core-collapse supernovae are fundamentally important quantities, and an estimate of  $E \sim 1 \times 10^{51}$  ergs has often been used in calculating nucleosynthesis (e.g., Woosley & Weaver 1995; Thielemann et al. 1996) and the impact on the interstellar medium. (In the present paper, we use the explosion energy  $E$  for the final kinetic energy of explosion.) A good example of this estimate is SN1987A in the Large Magellanic Cloud, whose energy is estimated to be  $E = (1.0 - 1.5) \times 10^{51}$  ergs from its early light curve (Shigeyama et al. 1987, 1988; Woosley et al. 1988; Arnett et al. 1989; Nakamura et al. 1998; Blinnikov et al. 2000).

SN1998bw called into question the applicability of the above energy estimate for all core-collapse supernovae. This supernova was discovered in the error box of the

gamma-ray burst GRB980425 (Soffitta et al. 1998; Lidman et al. 1998; Galama et al. 1998). Although the association of supernovae with gamma-ray bursts is still the subject of controversy (e.g., Wang & Wheeler 1998; Norris et al. 1999), SN1998bw is a quite unusual supernova in its radio and optical properties (Galama et al. 1998; Iwamoto et al. 1998; Kulkarni et al. 1998). It is one of the most luminous supernovae at radio wavelengths and its peak luminosity was attained exceptionally early in comparison with other radio supernovae (Kulkarni et al. 1998). From the optical spectra SN1998bw is classified as a Type Ic supernova (SN Ic), but it shows unusually broad spectral features. The modeling of the early light curve and spectra leads us to conclude that it was an explosion of a  $\sim 14 M_{\odot}$  C + O star with the explosion energy  $E = 3 - 6 \times 10^{52}$  ergs, which is about thirty times larger than that of a canonical supernova (Iwamoto et al. 1998; Woosley, Eastman & Schmidt 1999; Branch 2000; Nakamura et al. 2000, 2001). The amount of  $^{56}\text{Ni}$  ejected from SN1998bw is found to be  $M(^{56}\text{Ni}) \simeq 0.4 - 0.7 M_{\odot}$  (Nakamura et al. 2000, 2001; Sollerman et al. 2000), which is about 10 times larger than the  $0.07 M_{\odot}$  produced in SN1987A, a typical value for core-collapse supernovae.

We have used the term 'hypernova' to describe such an extremely energetic supernova with  $E \gtrsim 10^{52}$  ergs (Nomoto et al. 2000). In terms of explosion energies,

<sup>1</sup>Department of Astronomy, School of Science, University of Tokyo, Tokyo, Japan; nakamura@astron.s.u-tokyo.ac.jp<sup>2</sup>Department of Astronomy, School of Science, University of Tokyo, Tokyo, Japan; umeda@astron.s.u-tokyo.ac.jp<sup>3</sup>Department of Physics, College of Science and Technology, Nihon University, Tokyo, Japan; iwamoto@etoile.phys.cst.nihon-u.ac.jp<sup>4</sup>Department of Astronomy, School of Science, University of Tokyo, Tokyo, Japan; nomoto@astron.s.u-tokyo.ac.jp<sup>5</sup>Department of Physics, School of Sciences, University of Kyushu, Fukuoka, Japan; hashi@gemini.rc.kyushu-u.ac.jp<sup>6</sup>Department of Physics and Astronomy, University of Tennessee, Knoxville, TN 37996-1200 and Physics Division, Oak Ridge National Laboratory, Oak Ridge, TN 37831-6354 and Joint Institute for Heavy Ion Research, Oak Ridge National Laboratory, Oak Ridge, TN 37831-6374, USA; raph@mail.phy.ornl.gov<sup>7</sup>Department für Physik und Astronomie, Universität Basel, Switzerland; fkt@quasar.physik.unibas.ch<sup>8</sup>Research Center for the Early Universe, School of Science, University of Tokyo, Tokyo, Japan

pair-instability supernovae of  $150 - 200 M_{\odot}$  stars also explode with  $E \gtrsim 10^{52}$  ergs, thus being called hypernovae (e.g., Ober et al. 1983; Bond et al. 1984; Stringfellow & Woosley 1988). In the present paper, we concentrate on nucleosynthesis in core-collapse hypernovae.

Recently, other hypernovae candidates have been recognized. SN1997ef and SN1998ey are also classified as SNe Ic, and show very broad spectral features similar to SN1998bw (Garnavich et al. 1997, 1998). The spectra and the light curve of SN1997ef have been well simulated by the explosion of a  $10M_{\odot}$  C+O star with  $E = 1.0 \pm 0.2 \times 10^{52}$  ergs and  $M(^{56}\text{Ni}) \sim 0.15 M_{\odot}$  (Iwamoto et al. 2000; Mazzali, Iwamoto, & Nomoto 2000). SN1997cy is classified as a SN IIn and unusually bright (Germany et al. 2000; Turatto et al. 2000). Its light curve has been simulated by a circumstellar interaction model which requires  $E \sim 5 \times 10^{52}$  ergs (Turatto et al. 2000). The spectral similarity of SN1999E to SN1997cy (Cappellaro et al. 1999) would suggest that SN1999E is also a hypernova. Note that all of these estimates of  $E$  assume a spherically symmetric event.

In this paper, we explore nucleosynthesis in such energetic core-collapse induced supernovae, the systematic study of which has not yet been done. In §2, we briefly describe the argument that the progenitor mass  $M$  and explosion energy  $E$  are very large from the observation of SN1998bw. In §3 and §4, the characteristics of nucleosynthesis in hypernovae are investigated with detailed nucleosynthesis calculations and compared with nucleosynthesis in canonical supernovae. We also discuss possible effects on the Galactic chemical evolution and on the abundances in metal-poor stars in §5. A summary is given in section 6.

## 2. THE PROGENITOR OF SN1998BW

In this section, we will use SN1998bw, the first discovered hypernova, to describe how one can constrain the progenitor mass  $M$  and the explosion energy  $E$  from the observed light curve width and the peak luminosity by using the relation between  $M$ ,  $E$  and the synthesized  $^{56}\text{Ni}$  mass  $M(^{56}\text{Ni})$ . The light curve of SN1998bw (Galama et al. 1998) showed a very early rise and reached the peak luminosity at  $\sim 18$  days after the explosion before declining exponentially with time. This decline clearly indicates that the light curve is powered by the radioactive decay of  $^{56}\text{Ni}$  and  $^{56}\text{Co}$  as in usual SNe. The distance to the host galaxy ESO184-G82 is estimated to be  $\sim 37.8$  Mpc (Patat et al. 2001). From this distance, the peak absolute luminosity is estimated to be  $\sim 1 \times 10^{43}$  ergs  $\text{s}^{-1}$ , which is about ten times larger than previous SNe II or SNe Ib/c (e.g., SN1994I; Nomoto et al. 1994; Iwamoto et al. 1994), and as bright as an average SN Ia. The ejected  $^{56}\text{Ni}$  mass necessary to achieve such a large luminosity is estimated to be  $0.4 - 0.7 M_{\odot}$ , which is also about ten times larger than those of typical core-collapse SNe.

The peak width of the light curve,  $\tau_{\text{peak}}$ , is approximately related to the mass of the ejecta  $M_{\text{ej}}$  and  $E$  as follows.

$$\tau_{\text{peak}} \sim \sqrt{\tau_{\text{diff}} \cdot \tau_{\text{dyn}}} \sim \left(\frac{\kappa}{c}\right)^{1/2} M_{\text{ej}}^{3/4} E^{-1/4}, \quad (1)$$

where  $\kappa$  is the opacity and  $c$  is the speed of light. This relation is derived from multiplying the time scale of photo-

ton diffusion  $\tau_{\text{diff}} \sim \kappa \rho R^2 / c$  with the dynamical time scale  $\tau_{\text{dyn}} \sim R/v$  (Arnett 1982, 1996). This means that we can determine only  $M_{\text{ej}}^3/E$  by the light curve fitting. However, the information about the photospheric velocity can be used to break the degeneracy. In fact, Iwamoto et al. (1998) and Nakamura et al. (2000, 2001) used the photospheric velocity to constrain  $M_{\text{ej}}^{1/2}/E^{1/2}$  and determined  $M_{\text{ej}}$  and  $E$  as  $M_{\text{ej}} \sim 10 - 11 M_{\odot}$  and  $E \sim 3 - 6 \times 10^{52}$  ergs. From this ejecta mass and spectral type (Ic), they also concluded that the progenitor of SN1998bw was a C + O star with mass of  $\sim 14 M_{\odot}$ , corresponding to an initial main-sequence mass  $\sim 40 M_{\odot}$ . This is relatively large compared with determinations of  $\sim 20 M_{\odot}$  for SN1987A (Arnett et al. 1989; Shigeyama & Nomoto 1990),  $\sim 13 M_{\odot}$  for SN1993J (Nomoto et al. 1993a; Woosley et al. 1994), and  $\sim 14 M_{\odot}$  for SN1994I (Nomoto et al. 1994; Iwamoto et al. 1994; Young et al. 1995).

We can also exclude conventional masses of progenitors without using the information from photospheric velocities, but instead utilizing the peak luminosity, i.e.,  $M(^{56}\text{Ni})$ . The products of explosive burning are largely determined by the maximum temperature behind the shock,  $T_s$ . Material which experiences  $T_s > 5 \times 10^9$  K undergoes complete Si-burning, forming predominantly  $^{56}\text{Ni}$ . We can estimate the radius of the sphere in which  $^{56}\text{Ni}$  is dominantly produced as

$$R_{\text{Ni}} \sim 3700 (E/10^{51} \text{ergs})^{1/3} \text{ km}, \quad (2)$$

which is derived from  $E = 4\pi/3 R_{\text{Ni}}^3 a T_s^4$  with  $T_s = 5 \times 10^9 \text{ K}$  (e.g., Thielemann et al. 1996). Note that equation (1) indicates that smaller  $M_{\text{ej}}$  correspond to smaller  $E$  for a given  $\tau_{\text{peak}}$ , while equation (2) relates a smaller  $E$  to smaller  $R_{\text{Ni}}$ . Thus, combining these two equations, we find that  $R_{\text{Ni}}$  is smaller for smaller  $M_{\text{ej}}$ . In other words, a small mass progenitor may not produce a significantly large amount of  $^{56}\text{Ni}$ .

Figure 1 shows the mass enclosed within a radius  $r$  of the pre-collapse stars for stellar masses of  $M = 13 - 40 M_{\odot}$  (Nomoto et al. 1993b). We can see that the stellar structure actually provides the above relation, i.e., smaller  $M_{\text{ej}}$  corresponding to a smaller amount of  $R_{\text{Ni}}$ . A less massive star contains a smaller amount of mass in the same radius. Therefore, a less massive star ejects a smaller amount of  $^{56}\text{Ni}$  than a more massive star, when they are subjected to explosions of the same energy.

For SN1998bw,  $0.4 - 0.7 M_{\odot}$   $^{56}\text{Ni}$  is ejected. Since the mass of a collapsed star (neutron star or black hole) is at least as large as the mass of the pre-collapse Fe core, being  $1.2 - 1.9 M_{\odot}$  as indicated in Figure 1, the mass contained within  $R_{\text{Ni}}$  should exceed  $\sim 1.6 - 2.3 M_{\odot}$ . For example, consider an explosion of a  $6M_{\odot}$  C+O star, corresponding to a main-sequence mass  $\sim 25 M_{\odot}$ . If such a C+O star explodes, the ejecta mass becomes  $M_{\text{ej}} \lesssim 4.4 M_{\odot}$ , which, along with the light curve equation (1), yields  $E \lesssim 2 \times 10^{51}$  ergs. Substituting  $E \lesssim 2 \times 10^{51}$  ergs for equation (2), we obtain  $R_{\text{Ni}} \lesssim 4700 \text{ km}$ . Within this  $R_{\text{Ni}}$ , only  $1.8 M_{\odot}$  is enclosed (Figure 1), so that only  $0.2 M_{\odot}$   $^{56}\text{Ni}$  can be ejected. From this, we exclude the models less massive than  $25 M_{\odot}$  in their main sequence because they cannot eject enough  $^{56}\text{Ni}$ . This argument above is further evidence that the progenitor of SN1998bw is a massive star.

Since the progenitor of another hypernova candidate SN1997ef also seems to be massive (Iwamoto et al. 2000), we consider only relatively massive progenitor models ( $8 - 16 M_{\odot}$  He core models) in the following for nucleosynthesis calculations of hypernovae.

### 3. MODELS

Hypernovae are characterized by explosion energies larger than  $E \sim 10^{52}$  ergs. Such an energetic stellar explosion may be associated with the formation of a black hole as has been discussed in the context of the GRB-SNe connection (Woosley 1993; Paczynski 1998; Iwamoto et al. 1998; MacFadyen & Woosley 1999). In these models, the gravitational energy, or the rotational energy would be released via pair-neutrino annihilation or the Blandford-Znajek mechanism (Blandford & Znajek 1977). Alternatively, large magnetic energies are released from a possible magnetar (Nakamura 1998; Wheeler et al. 2000). The explosion may also be aspherical (Höflich, Wheeler, & Wang 1999; MacFadyen & Woosley 1999; Khokhlov et al. 1999). However, the actual explosion mechanism and the degree of asphericity in the ejecta are still quite uncertain. For the present paper, therefore, we investigate nucleosynthesis in spherical explosions as an extreme case. In a next step, we will explore aspherical explosion models (Maeda et al. 2000; also Nagataki et al. 1997).

Our calculations are performed in the same way as studies of supernova nucleosynthesis (e.g., Hashimoto et al. 1989; Thielemann, Hashimoto, & Nomoto 1990; Hashimoto 1995; Thielemann, Nomoto, & Hashimoto 1996; Nakamura et al. 1999). First, the hydrodynamical simulations are performed with a one dimensional PPM (piecewise parabolic method) code (Colella & Woodward 1984), which includes a small nuclear reaction network that contains only 13 alpha nuclei ( $^4\text{He}$ ,  $^{12}\text{C}$ ,  $^{16}\text{O}$ ,  $^{20}\text{Ne}$ ,  $^{24}\text{Mg}$ ,  $^{28}\text{Si}$ ,  $^{32}\text{S}$ ,  $^{36}\text{Ar}$ ,  $^{40}\text{Ca}$ ,  $^{44}\text{Ti}$ ,  $^{48}\text{Cr}$ ,  $^{52}\text{Fe}$ , and  $^{56}\text{Ni}$ ) in order to take into account the energy release due to nuclear reactions. We generate a shock wave by depositing thermal energy below the mass cut, which divides the central compact object and the ejecta. Next, post-processing calculations are performed at each mesh point of the hydrodynamical model with an extended reaction network of 293 isotopes (Hix & Thielemann 1996, 1999) to provide precise total yields (even for minor abundances). The progenitor models are taken from Nomoto & Hashimoto (1988), Hashimoto (1995) and Nomoto et al. (1997). We make use of the  $6M_{\odot}$ ,  $8M_{\odot}$ ,  $10M_{\odot}$ , and  $16M_{\odot}$  He core models, which correspond approximately to the main sequence masses of  $20M_{\odot}$ ,  $25M_{\odot}$ ,  $30M_{\odot}$ , and  $40M_{\odot}$ , respectively. In order to compare nucleosynthesis in hypernovae with ordinary supernovae and also to investigate the dependence on the explosion energy, we study explosion energies of  $E = 100$ ,  $30$ ,  $10$ , and  $1 \times 10^{51}$  ergs. The mass cuts are summarized in Table 1. We chose these mass cuts to be as small as they can, but prevent O/Fe of the ejecta from being much less than the solar value (§5.1).

### 4. DEPENDENCE ON EXPLOSION ENERGY

Figure 2 shows nucleosynthesis in hypernovae and typical supernovae for  $E = 100$  (top left),  $30$  (top right),  $10$  (bottom left), and  $1 (bottom right) \times 10^{51}$  ergs. The progenitor is  $16M_{\odot}$  He core model. From this figure, we note

the following characteristics of nucleosynthesis with very large explosion energies.

- (1) The region of complete Si-burning, where  $^{56}\text{Ni}$  is dominantly produced, is extended to the outer, lower density region. How much mass is ejected from this region depends on the mass cut. The large amount of  $^{56}\text{Ni}$  observed in hypernovae (e.g.,  $\sim 0.4 - 0.7 M_{\odot}$  for SN1998bw and  $\sim 0.15M_{\odot}$  for SN1997ef) implies that the mass cut is rather deep, so that the elements synthesized in this region such as  $^{59}\text{Cu}$ ,  $^{63}\text{Zn}$ , and  $^{64}\text{Ge}$  (which decay into  $^{59}\text{Co}$ ,  $^{63}\text{Cu}$ , and  $^{64}\text{Zn}$ , respectively) are ejected more abundantly than in normal supernovae. (The mass fraction of  $^{63}\text{Zn}$  is so small,  $\lesssim 1 \times 10^{-5}$ , that  $^{63}\text{Zn}$  is out of range in Figure 2.) In the complete Si-burning region of hypernovae, elements produced by  $\alpha$ -rich freezeout are enhanced because nucleosynthesis proceeds at lower densities than in normal supernovae (Figure 3). Figure 2 clearly shows the trend that a larger amount of  $^4\text{He}$  is left for more energetic explosions. Hence, elements synthesized through capturing of  $\alpha$ -particles, such as  $^{44}\text{Ti}$ ,  $^{48}\text{Cr}$ , and  $^{64}\text{Ge}$  (decaying into  $^{44}\text{Ca}$ ,  $^{48}\text{Ti}$ , and  $^{64}\text{Zn}$ , respectively) are more abundant.
- (2) More energetic explosions produce a broader incomplete Si-burning region. The elements produced mainly in this region such as  $^{52}\text{Fe}$ ,  $^{55}\text{Co}$ , and  $^{51}\text{Mn}$  (decaying into  $^{52}\text{Cr}$ ,  $^{55}\text{Mn}$ , and  $^{51}\text{V}$ , respectively) are synthesized more abundantly with the larger explosion energy.
- (3) Oxygen and carbon burning takes place in more extended, lower density regions for the larger explosion energy. Therefore, the elements O, C, Al are burned more efficiently and the abundances of the elements in the ejecta are smaller, while a larger amount of burning products such as Si, S, and Ar is synthesized by oxygen burning.

Tables 2 - 9 summarize the nucleosynthesis products of hypernovae (and normal supernovae) before and after radioactive decays for various explosion energies. Major radioactive elements are summarized in table 10. The progenitors are He stars of  $16M_{\odot}$ ,  $10M_{\odot}$ ,  $8M_{\odot}$ , and  $6M_{\odot}$ . Products from the H-rich envelope are not included. Note that the amount of the elements produced in the complete Si-burning region depends on the mass cut. Here we choose the mass cuts shown in Table 1.

Figure 4 displays the abundances of stable isotopes relative to their solar values for  $E = 100$  (top left),  $30$  (top right),  $10$  (bottom left), and  $1 (bottom right) \times 10^{51}$  ergs. The progenitor is a  $16M_{\odot}$  He star. The isotopic ratios relative to  $^{16}\text{O}$  with respect to the solar values are shown. The nucleosynthesis is characterized by large abundance ratios of intermediate mass nuclei and heavy nuclei with respect to  $^{56}\text{Fe}$  for more energetic explosions, except for the elements O, C, Al which are consumed in oxygen and carbon burning. In particular, the amounts of  $^{44}\text{Ca}$  and  $^{48}\text{Ti}$  are increased significantly with increasing explosion energy because of the lower density regions which experience complete Si-burning through  $\alpha$ -rich freezeout. To see this more clearly, we add the isotopes and show in Figure 5 their ratios to oxygen relative to the solar values

for various explosion energies. We note that [C/O] and [Mg/O] are not sensitive to the explosion energy because C, O, and Mg are consumed by oxygen burning. On the other hand, [Si/O], [S/O], [Ti/O], and [Ca/O] are larger for larger explosion energies because Si and S are produced in the oxygen burning region, and Ti and Ca are increased in the enhanced  $\alpha$ -rich freezeout.

## 5. CONTRIBUTION OF HYPERNOVAE TO THE GALACTIC CHEMICAL EVOLUTION

Because of the small number of hypernovae so far observed, their occurrence frequency is difficult to estimate. However, their effects on the Galactic chemical evolution could be important because of their production of large amounts of heavy elements.

If hypernovae occurred in the early stage of the Galactic evolution, the abundance pattern of a hypernova may be observable in some low-mass halo stars. This results from the very metal-poor environment, where the heavy elements synthesized in a single hypernova (or a single supernova) dominate the heavy element abundance pattern (Audouze & Silk 1995). It is plausible that hypernova explosions induce star formations. The low-mass stars produced by this event should have the hypernova-like abundance pattern and still exist in the Galactic halo. The metallicity of such stars is likely to be determined by the ratio of ejected iron mass from the relevant hypernova to the mass of hydrogen gathered by the hypernova, which might be in the range range of  $-4 \lesssim [\text{Fe}/\text{H}] \lesssim -2.5$  ( $[\text{A}/\text{B}] = \log_{10}(\text{A}/\text{B}) - \log_{10}(\text{A}/\text{B})_{\odot}$ ; Ryan et al. 1996; Shigeyama & Tsujimoto 1998; Nakamura et al. 1999; Argast et al. 2000).

We also discuss the abundances of the black hole binary X-ray Nova Sco as a possible direct indication of hypernova nucleosynthesis.

### 5.1. Alpha-Elements and Ti relative to Fe

First of all, the most significant feature of hypernova nucleosynthesis is a large amount of Fe. One hypernova can produce 2 - 10 times more Fe than normal core-collapse supernovae, which is almost the same amount of Fe as produced in a SN Ia. This large iron production leads to small ratios of  $\alpha$  elements over iron in hypernovae (Figure 4). In this connection, the abundance pattern of the very metal-poor binary CS22873-139 ( $[\text{Fe}/\text{H}] = -3.4$ ) is interesting. This binary has only an upper limit to  $[\text{Sr}/\text{Fe}] < -1.5$ , and therefore was suggested to be a second generation star (Nordström et al. 2000; Spite et al. 2000). The interesting pattern is that this binary shows almost solar Mg/Fe and Ca/Fe ratios, as is the case with hypernovae (Figure 4) as pointed out by Umeda, Nomoto & Nakamura (2000). Another feature of CS22873-139 is enhanced Ti/Fe ( $[\text{Ti}/\text{Fe}] \sim +0.6$ ; Nordström et al. 2000; Spite et al. 2000), which could be explained by a hypernova explosion.

It has been pointed out that Ti is deficient in Galactic chemical evolution models using supernova yields currently available (e.g., Timmes et al. 1995; Thielemann et al. 1996), especially at  $[\text{Fe}/\text{H}] \lesssim -1$  when SNe Ia have not contributed to the chemical evolution. However, if the contribution from hypernovae to Galactic chemical evolution is relatively large (or supernovae are more energetic than the typical value of  $1 \times 10^{51}$  erg), this problem could be relaxed. As we have seen in the previous section, the

$\alpha$ -rich freezeout is enhanced in hypernovae because nucleosynthesis proceeds under the circumstance of lower densities and incomplete Si-burning occurs in more extended regions. Thus,  $^{40}\text{Ca}$ ,  $^{44}\text{Ca}$ , and  $^{48}\text{Ti}$  are produced and could be ejected into space more abundantly.

### 5.2. Iron-Peak Elements

McWilliam et al. (1995) and Ryan et al. (1996) found a peculiar abundance pattern in the iron-peak elements in metal-poor stars of  $[\text{Fe}/\text{H}] \lesssim -2$ . That is,  $[\text{Cr}/\text{Fe}]$  and  $[\text{Mn}/\text{Fe}]$  increase with increasing  $[\text{Fe}/\text{H}]$ , while  $[\text{Co}/\text{Fe}]$  shows the opposite trend and decrease. This trend cannot be explained with the conventional chemical evolution model that uses previous nucleosynthesis yields (e.g., Tsujimoto et al. 1995; Woosley & Weaver 1995).

Nakamura et al. (1999) have shown that this trend of decreasing Cr and Mn with increasing Co is reproduced by decreasing the mass cut between the ejecta and the collapsed star for the same explosion model. This is because Co is mostly produced in complete Si-burning regions, while Mn and Cr are mainly produced in the outer incomplete Si-burning region. If the mass cut is located at smaller  $M_r$ , the mass ratio between the complete and incomplete Si-burning region is larger. Therefore, mass cuts at smaller  $M_r$  increase the Co fraction but decrease the Mn and Cr fractions in the ejecta. Nakamura et al. (1999) have also shown that the observed trend with respect to  $[\text{Fe}/\text{H}]$  may be explained if the mass cut tends to be smaller in  $M_r$  for the larger mass progenitor.

Here, we investigate whether the observed trend of these iron-peak elements in metal-poor stars can be explained with the the abundance pattern of hypernovae. In Table 11, we summarize the abundance ratios of iron-peak elements in the ejecta. In Figure 6, we plot  $[\text{Mn}/\text{Fe}]$  vs.  $[\text{Co}/\text{Fe}]$  and  $[\text{Cr}/\text{Fe}]$  for the  $16 M_{\odot}$  He star models with  $E = (1 - 30) \times 10^{51}$  ergs, and  $8 M_{\odot}$  He star models with  $E = (1 - 10) \times 10^{51}$  ergs. This figure clearly shows the correlation between  $[\text{Mn}/\text{Fe}]$  and  $[\text{Cr}/\text{Fe}]$ , and anti-correlation between  $[\text{Mn}/\text{Fe}]$  and  $[\text{Co}/\text{Fe}]$ , which are the same trends as observed in the metal-poor stars.

To understand the dependence on  $E$ , let us compare the models with  $1 \times 10^{51}$  ergs and  $10 \times 10^{51}$  ergs which have almost the same mass cut (Table 1). In the model with  $E = 10 \times 10^{51}$  ergs, both complete and incomplete Si-burning regions shift outward in mass compared with  $E = 1 \times 10^{51}$  ergs because of a larger explosion energy. Thus, the model with larger  $E$  has a larger mass ratio between the complete and incomplete Si-burning regions. This relation between  $E$  and the mass ratio does not hold if the explosion energy is too large. For example, in the  $16 M_{\odot}$  He star models with  $100 \times 10^{51}$  ergs and  $8 M_{\odot}$  He star models with more than  $30 \times 10^{51}$  ergs, incomplete Si-burning extends so far out that Mn and Cr increase too much to fit the metal-poor star data. For this reason, we do not include these models in Figure 6.

In metal-poor stars,  $[\text{Mn}/\text{Fe}]$  increases with  $[\text{Fe}/\text{H}]$ . Hypernova yields are consistent with this trend if hypernovae with larger  $E$  induce the formation of stars with smaller  $[\text{Fe}/\text{H}]$ . This supposition is reasonable because the mass of interstellar hydrogen gathered by a hypernova is roughly proportional to  $E$  (Cioffi et al. 1988; Shigeyama & Tsujimoto 1998) and the ratio of the ejected iron mass to  $E$  is smaller for hypernovae than for canonical supernovae.

The amounts of iron-peak elements and their ratios in the ejecta of hypernovae depend on the mass cut that is still uncertain. How the abundance ratios depend on the mass cut is discussed in Umeda & Nomoto (2001). If we adopt a smaller mass cut, a larger amount of  $^{56}\text{Ni}$  is ejected and the abundance ratios can be different from Table 11. To reduce the uncertainty in the prediction, it is necessary to observe more hypernovae. We can determine the amount of  $^{56}\text{Ni}$  ejected from a hypernova by the light curve and spectral fitting (e.g., Iwamoto et al. 2000). Combining this information with nucleosynthesis calculations, we can estimate the mass cut as in the case of SN1998bw (Nakamura et al. 2001).

### 5.3. Abundances in Starburst Galaxies

X-ray emissions from the starburst galaxy M82 were observed with ASCA and the abundances of several heavy elements were obtained (Tsuru et al. 1997). Tsuru et al. (1997) found that the overall metallicity of M82 is quite low, i.e., O/H and Fe/H are only 0.06 - 0.05 times solar, while Si/H and S/H are  $\sim 0.40$  - 0.47 times solar. This implies that the abundance ratios are peculiar, i.e., the ratio O/Fe is about solar, while the ratios of Si and S relative to O and Fe are as high as  $\sim 6$  - 8. These ratios are very different from those ratios in SNe II. The age of M82 is estimated to be  $\lesssim 10^8$  years, which is too young for Type Ia supernovae to contribute to enhance Fe relative to O. Tsuru et al. (1997) also estimated that the explosion energy required to produce the observed amount of hot plasma per oxygen mass is significantly larger than that of normal SNe II (here the oxygen mass dominates the total mass of the heavy elements). Tsuru et al. (1997) thus concluded that neither SN Ia nor SN II can reproduce the observed abundance pattern of M82.

Compared with normal SNe II, the important characteristic of hypernova nucleosynthesis is the large Si/O, S/O, and Fe/O ratios. Quantitatively, the enhancement of Si and S over O in our current hypernova models are smaller than those observed in M82, but possible aspherical effects might enhance the Si/O and S/O ratios over the spherical models. Also, the larger Si/O and S/O ratios are yielded, if the progenitors of hypernovae have smaller metallicities (Nakamura et al. 2000). Hypernovae could also produce larger  $E$  per oxygen mass than normal SNe II. We therefore suggest that hypernova explosions may make important contributions to the metal enrichment and energy input to the interstellar matter in M82. If the IMF of the star burst is relatively flat compared with Salpeter IMF, the contribution of very massive stars and thus hypernovae could be much larger than in our Galaxy.

### 5.4. Abundances in a Black Hole Binary

X-ray Nova Sco (GRO J1655-40), which consists of a massive black hole and a low mass companion (e.g., Brandt et al. 1995; Nelemans et al. 2000), also exhibits what could be the nucleosynthesis signature of a hypernova explosion. The companion star is enriched with Ti, S, Si, Mg, and O but not much Fe (Israelian et al. 1999). This is compatible with heavy element ejection from a black hole progenitor. In order to eject large amount of Ti, S, and Si and to have at least  $\sim 4 M_{\odot}$  below mass cut and thus form a massive black hole, the explosion would need to be highly energetic (Figure 2; Israelian et al. 1999; Brown

et al. 2000; Podsiadlowski et al. 2000). A hypernova explosion with the mass cut at large  $M_r$  ejects a relatively small mass Fe and would be consistent with these observed abundance features. Alternatively, if the explosion which resulted from the formation of the black hole in Nova Sco was asymmetric, then it is likely that the companion star captured material ejected in the direction away from the strong shock which contained relatively little Fe compared with the ejecta in the strong shock (Maeda et al. 2000).

## 6. SUMMARY

We investigated explosive nucleosynthesis in hypernovae, that is, hyper-energetic supernovae. Detailed nucleosynthesis calculations were performed and compared to those of ordinary core-collapse supernovae. We also studied implications to Galactic chemical evolution and the abundances in metal-poor stars.

We demonstrated, using the SN1998bw data, that progenitor of hypernovae must be massive based on the information from light curve and nucleosynthesis calculations of  $^{56}\text{Ni}$ , without using spectral information. This argument is useful for cases where reliable spectral information is not available.

In hypernovae, both complete and incomplete Si-burning takes place in more extended, and hence, lower density regions, so that the alpha-rich freezeout is enhanced in comparison with normal supernova nucleosynthesis. Thus  $^{44}\text{Ca}$ ,  $^{48}\text{Ti}$ , and  $^{64}\text{Zn}$  are produced more abundantly than in canonical supernovae. Oxygen and carbon burning also takes place in more extended regions for the larger explosion energy, hence the yield of these fuel elements are smaller than canonical supernovae.

We found that hypernova nucleosynthetic yields are compatible with the observed Cr, Mn, and Fe abundances of metal-poor halo stars, provided that the explosion energy is  $\sim 10^{52}$  ergs. Our results imply that heavier progenitors allow larger explosion energy to match the abundance pattern of metal-poor stars, although further investigations are necessary for firm conclusion. Our results suggest that some metal-poor halo stars may bear the abundance pattern of a single hypernova.

We also suggest that the problem of the deficit of Ti in the Galactic chemical evolution with the supernova yields currently available could be settled by the contribution of hypernovae, in which  $\alpha$ -rich freezeout is enhanced and large amounts of  $\alpha$ -elements are ejected. The abundance pattern of the starburst galaxy M82, characterized by abundant Si and S relative to O and Fe, may be attributed to hypernova explosions if the IMF is relatively flat, and thus the contribution of massive stars to the galactic chemical evolution is large. The black hole binary X-ray Nova Sco (GRO J1655-40) may also be affected by a hypernova explosion, which can eject large amount of Ti, S, and Si and leave a massive black hole as a compact remnant.

In this paper, we performed calculations assuming spherical symmetry and thus did not take account of non-spherical effects. For example, if a jet is associated with hypernovae, the explosive shock may be pointed and stronger in this direction. In this case, the high explosion energies along the jet should have the properties of nucleosynthesis in hypernovae discussed above and orthogonal to the jet may be more like ordinary supernovae. In such

conditions, a hypernova could make ejecta which have a range of abundance ratios (as seen in Figure 6) in different directions. If those ejecta in various directions interact with interstellar matter and form mixed materials of various mass ratios, stars which could form from such interactions would have a range of metallicity and abundance ratios among iron-peak elements. For example, the ejecta in the jet direction has larger amount of complete Si-burning products (i.e., larger [Co/Fe]) and are mixed with larger amount of hydrogen (i.e., producing smaller [Fe/H]) because of higher velocities than in other directions. Then such explosions might be responsible for the abundance trends in the metal-poor stars. Multi-dimensional simulations are needed to investigate these possibilities.

We would like to thank Drs. B. Nordström, F. Spite, T. Tsuru, G. Israelian, G. Brown, Ph. Podsiadlowski, P. Mazzali, and B. Schmidt for stimulating discussion on the observational indication of hypernova nucleosynthesis. This work has been supported in part by the Grant-in-Aid for Scientific Research (12640233, 12740122) and COE research (07CE2002) of the Japanese Ministry of Education, Science, Culture, and Sports, Swiss National Science Foundation grant 2000-53798.98, U.S. National Aeronautics and Space Administration grant NAG5-8405 and the Joint Institute for Heavy Ion Research, which has as member institutions the University of Tennessee, Vanderbilt University, and the Oak Ridge National Laboratory. ORNL is managed by UT-Battelle, LLC, for the U.S. Department of Energy under contract DE-AC05-00OR22725.

## REFERENCES

Argast, D., Salmand, M., Gerhard, O.E., & Thielemann, F.-K. 2000, *A&A*, 356, 873

Arnett, W. D. 1982, *ApJ*, 253, 785

Arnett, W. D. 1996, *Supernovae and Nucleosynthesis* (Princeton: Princeton University Press)

Arnett, W. D., Bahcall, J. N., Kirshner, R. P., & Woosley, S. E. 1989, *ARA&A*, 27, 629

Audouze, J., & Silk, J. 1995, *ApJ*, 451, L49

Blandford, R.D., & Znajek, R.L. 1977, *MNRAS*, 179, 433.

Blinnikov, S., Lundqvist, P., Bartunov, O., Nomoto, K., & Iwamoto, K. 2000, *ApJ*, 532, 1132

Bloom, J. S., Kulkarni, S. R., Harrison, F., Prince, T., & Phinney, E. S. 1998, *ApJ*, 506, L105

Branch, D. 2000, in *Supernovae and Gamma Ray Bursts*, ed. M. Livio et al. (Cambridge: Cambridge University Press), in press

Bond, J. R., Arnett, W. D., & Carr, B. J. 1984, *ApJ*, 280, 825

Brandt, W.N., Podsiadlowski, Ph., & Sigurdsson, S. 1995, *MNRAS*, 277, L35

Brown, G.E., Lee, C.-H., Wijers, R.A.M.J., Lee, H.K., Israelian, G., & Bethe, H.A. 2000, *New Astronomy*, 5, 191

Cappellaro, E., Turatto, M., & Mazzali, P. 1999, *IAU Circ.* 7091

Cioffi, D.F., McKee, C.F., & Bertschinger, E. 1988, *ApJ*, 334, 252

Coellela, P., & Woodward, P. R. 1984, *J. Comput. Phys.* 54, 174

Galama, T. J., Vreeswijk, P. M., Van Paradijs, J., Kouveliotou, C., Augusteijn, T., Bohnhardt, H., Brewer, J. P., Doublier, V., Gonzalez, J.-F., Leibundgut, B., Lidman, C., Hainaut, O. R., Patat, F., Heise, J., in't Zand, J., Hurley, K., Groot, P. J., Strom, R. G., Mazzali, P. A., Iwamoto, K., Nomoto, K., Umeda, H., Nakamura, T., Young, T.R., Suzuki, T., Shigeyama, T., Koshut, T., Kippen, M., Robinson, C., de Wildt, P., Wijers, R. A. M. J., Tanvir, N., Greiner, J., Pian, E., Palazzi, E., Frontera, F., Masetti, N., Nicastro, L., Feroci, M., Costa, E., Piro, L., Peterson, B. A., Tinney, C., Boyle, B., Cannon, R., Stathakis, R., Sadler, E., Begam, M. C., & Ianna, P. 1998, *Nature*, 395, 670

Garnavich, P., Jha, S., Kirshner, R., Berlind, P. 1998, *IAU Circ.* 7066

Garnavich, P., Jha, S., Kirshner, R., Challis, P., Balam, D., Berlind, P., Thorstensen, J. & Macri, L. 1997, *IAU Circ.* 6798

Germany, L.M., Reiss, D.J., Schmidt, B.P., Stubbs, C.W., Sadler, E.M. 2000, *ApJ*, 533, 320

Hashimoto, M. 1995, *Prog. Theor. Phys.*, 94, 663

Hashimoto, M., Nomoto, K., & Shigeyama, T. 1989, *A&A*, 210, 5

Hix, W. R. & Thielemann, F.-K. 1996, *ApJ*, 460, 869

Hix, W. R. & Thielemann, F.-K. 1999, *ApJ*, 511, 862

Höflich, P., Wheeler, J. C., & Wang, L., 1999, *ApJ*, 521, 179

Israelian, G., Rebolo, R., Basri, G., Casares, J., & Martin, E.L. 1999, *Nature*, 401, 142

Iwamoto, K., Mazzali, P. A., Nomoto, K., Umeda, H., Nakamura, T., Patat, F., Danziger, I. J., Young, T. R., Suzuki, T., Shigeyama, T., Augusteijn, T., Doublier, V., Gonzalez, J.-F., Boe hnhardt, H., Brewer, J., Hainaut, O.R., Lidman, C., Leibundgut, B., Cappellaro, E., Turatto, M., Galama, T. J., Vreeswijk, P. M., Kouveliotou, C., Paradijs, J.van, Pian, E., Palazzi, E., & Frontera F. 1998, *Nature*, 395, 672

Iwamoto, K., Nakamura, T., Nomoto, K., Mazzali, P. A., Garnavich, P., Kirshner, R., Jha, S., Balam, D. & Thorsternsen, J. 2000, *ApJ*, 534, 660

Iwamoto, K., Nomoto, K., Höflich, P., Yamaoka, H., Kumagai, S., & Shigeyama, T., 1994, *ApJ*, 437, L115

Khokhlov, A. M., Höflich, P. A., Oran, E. S., Wheeler, J. C., Wang, L., & Chtchelkanova, A. Yu. 1999, *ApJ*, 524, L107

Kulkarni, S. R., Frail, D. A., Wieringa, M. H., Ekers, R. D., Sadler, E. M., Wark, R. M., Higdon, J. L., Phinney E. S., & Bloom, J. S. 1998, *Nature*, 395, 663

Lidman, C. et al. 1998, *IAU Circ.* 6895

MacFadyen, A.I. & Woosley, S.E. 1999, *ApJ*, 524, 262

Maeda, K., Nakamura, T., Nomoto, K., Mazzali, P. A., Pata, F., & Hachisu, I. 2000, *ApJ*, submitted (astro-ph/0011003)

Mazzali, P.A., Iwamoto, K., & Nomoto, K. 2000, *ApJ*, 545, 407

McWilliam, A., Preston, G.W., Sneden, C., & Searle, L. 1995, *AJ*, 109, 2757

Nagataki, S., Hashimoto, M., Sato, K., & Yamada, S. 1997, *ApJ*, 486, 1026

Nakamura, T. 1998, *Prog. Theor. Phys.*, 100, 921

Nakamura, T., Iwamoto, K., & Nomoto, K. 1998, in *Origin of Matter and Evolution of Galaxies in the Universe*, eds. T. Kajino, & S. Kubono (Singapore: World Scientific Publishing), 386

Nakamura, T., Maeda, K., Iwamoto, K., Suzuki, T., Nomoto, K., Mazzali, P.A., Turatto, M., Danziger, I.J., & Patat, N. 2000, in *IAU Symp.* 195, *Highly Energetic Physical Processes and Mechanisms for Emission from Astrophysical Plasmas*, eds. P. Martens, S. Tsuruta, & M. Weber (PASP), 347

Nakamura, T., Mazzali, P. A., Nomoto, K., & Iwamoto, K. 2001, *ApJ*, 550, in press (astro-ph/0007010)

Nakamura, T., Umeda, H., Nomoto, K., Thielemann, F.-K., & Burrows, A. 1999, *ApJ*, 517, 193

Nelemans, G., Tauris, T.M., & van den Heuvel, E.P.J. 2000, *A&A*, 352, 87

Nomoto, K. & Hashimoto, M. 1988, *Phys. Rep.*, 256, 173

Nomoto, K., Hashimoto, M., Tsujimoto, T., Thielemann, F.-K., Kishimoto, N., Kubo, Y., & Nakasato, N. 1997, *Nuclear Phys.*, A616, 79c

Nomoto, K., Iwamoto, K., Tsujimoto, T., & Hashimoto, M. 1993b, in *Frontiers of Neutrino Astronomy*, ed. Y. Suzuki and K. Nakamura (Tokyo: Universal Academy press), 235.

Nomoto, K., Mazzali, P.A., Nakamura, T., Iwamoto, K., Maeda, K., Suzuki, T., Turatto, M., Danziger, I.J., & Patat, F. 2000, in *Supernovae and Gamma Ray Bursts*, ed. M. Livio et al. (Cambridge: Cambridge University Press), in press (astro-ph/0003077)

Nomoto, K., Suzuki, T., Shigeyama, T., Kumagai, S., Yamaoka, H., Saio, H. 1993a, *Nature*, 364, 507

Nomoto, K., Yamaoka, H., Pols, O. R., van den Heuvel, E. P. J., Iwamoto, K., Kumagai, S., & Shigeyama, T. 1994, *Nature*, 371, 227

Nordström, B. et al. 2000, in *The First Stars (MPA/ESO Astrophysics Symposia)*, eds. A. Weiss, T. Abel, & V. Hill (Berlin: Springer), 76

Norris, J. P., Bonnell, J. T., & Watanabe, K. 1999, 518, 901

Ober, W. W., El Elid, M. F., Fricke, K. J. 1983, *A&A*, 1983, 119, 61

Paczynski, B. 1998, *ApJ*, 494, L45

Patat, F. et al., 2001, *ApJ*, in press (astro-ph/0103111)

Podsiadlowski, Ph., Nomoto, K., Maeda, K., Nakamura, T., Mazzali, P.A., & Schmidt, B. 2000, preprint

Ryan, S.G., Norris, J.E., & Beers, T.C. 1996, *ApJ*, 471, 254

Shigeyama, T., & Nomoto, K., 1990, *ApJ*, 360, 242

Shigeyama, T., Nomoto, K., & Hashimoto, M. 1988, *A&A*, 196, 141

Shigeyama, T., Nomoto, K., Hashimoto, M., & Sugimoto, D. 1987, *Nature*, 328, 320

Shigeyama, T. & Tsujimoto, T. 1998, *ApJ*, 507, L139

Soffitta, P., Feroci, M., & Poro. L. 1998, *IAU Circ.* 6884

Sollerman, J., Kozma, C., Fransson, C., Leibundgut, B., Lundqvist, P., Ryde, F., & Woudt, P. 2000, *ApJ* 537, L127

Spite, M., Depagne, E., Nordström, B., Hill, V., Cayrel, R., Spite, F., & Beers, T.C. 2000, *A&A*, 360, 1077

Stringfellow, G. S. & Woosely, S. E. 1988, Origin and Distribution of the elements, ed. G.J. Mathews (Singapore: World Scientific Publishing), 467

Thielemann, F.-K., Hashimoto, M., & Nomoto, K. 1990, *ApJ*, 349, 222

Thielemann, F.-K., Nomoto, K., & Hashimoto, M. 1996, *ApJ*, 460, 408

Thielemann, F.-K., Rauscher, T., Freiburghaus, C., Nomoto, K., Hashimoto, M., Pfeiffer, B., Kratz, K.-L. 1998, in Nucleosynthesis Basics and Applications to Supernovae, Nuclear and Particle Astrophysics, eds. J. Hirsch & D. Page (Cambridge: Cambridge University Press), 27

Tsujimoto, T., Nomoto, K., Yoshii, Y., Hashimoto, M., Yanagida, Y., & Thielemann, F.-K. 1995, *MNRAS*, 277, 945

Tsuru, T. G., Awaki, H., Koyama K., Ptak, A. 1997, *PASJ*, 49, 619

Turatto, M., Suzuki, T., Mazzali, P.A., Benetti, S., Cappellaro, E., Nomoto, K., Nakamura, T., Young, T.R., Patat, F. 2000, *ApJ*, 534, L57

Umeda, H., Nomoto, K. 2001, *ApJ*, submitted (astro-ph/0103241)

Umeda, H., Nomoto, K., & Nakamura, T. 2000, in The First Stars (MPA/ESO Astrophysics Symposia), eds. A. Weiss, T. Abel, & V. Hill (Berlin: Springer), 121

Wang, L., & Wheeler, J. C. 1998, *ApJ*, 504, L87

Wheeler, J. C., Yi, I., Höflich, P. A., & Wang, L. 2000, *ApJ*, 537, 810

Woosley, S. E., 1993, *ApJ*, 405, 273

Woosley, S. E., Eastman, R. G., & Schmidt, B. P. 1999, *ApJ*, 516, 788

Woosley, S. E., Eastman, R. G., Weaver, T. A., & Pinto, P.A. 1994, *ApJ*, 429, 300

Woosley, S. E., Pinto, P. A., & Enzman, L. 1988, *ApJ*, 324, 466

Woosley, S. E., & Weaver, T. A. 1995, *ApJS*, 101, 181

Young, T. R., Baron, E., & Branch, D. 1995, *ApJ*, 449L, 51

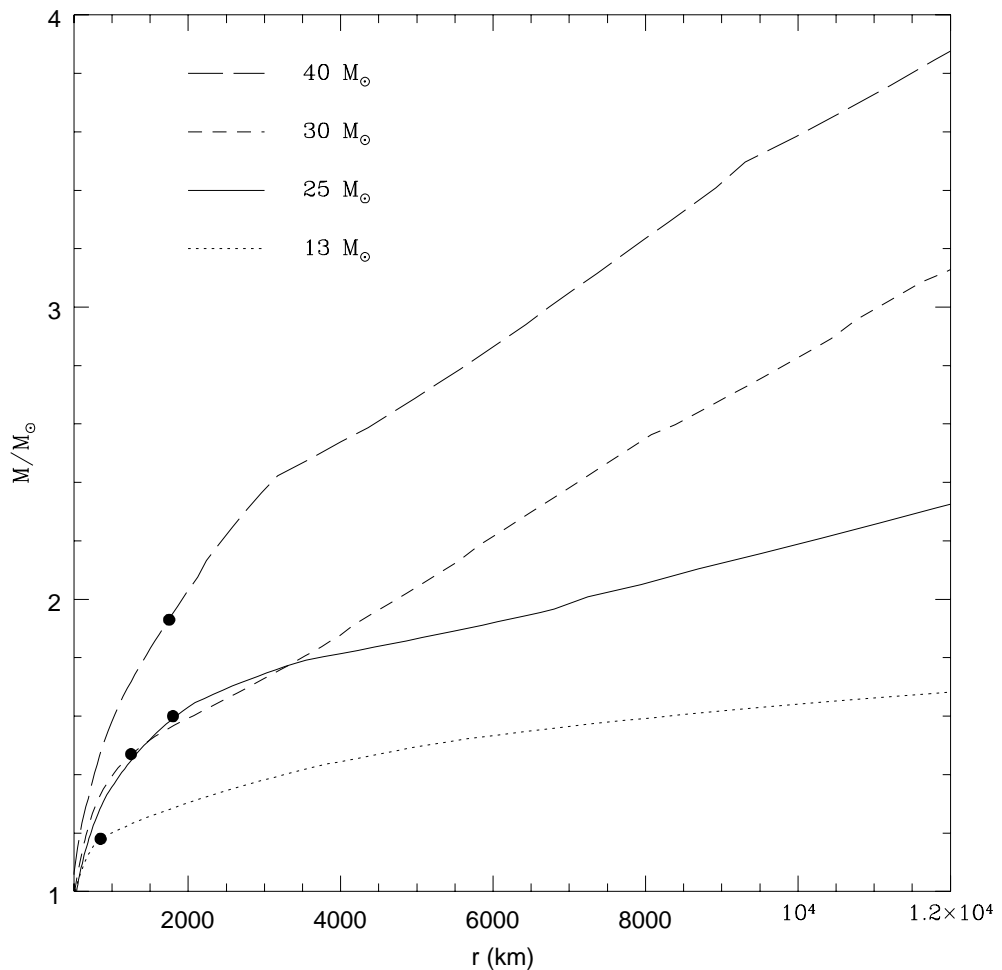


FIG. 1.— The mass enclosed within a radius  $r$  of the pre-collapse stars. Filled circles locate the position of the pre-collapse Fe core.

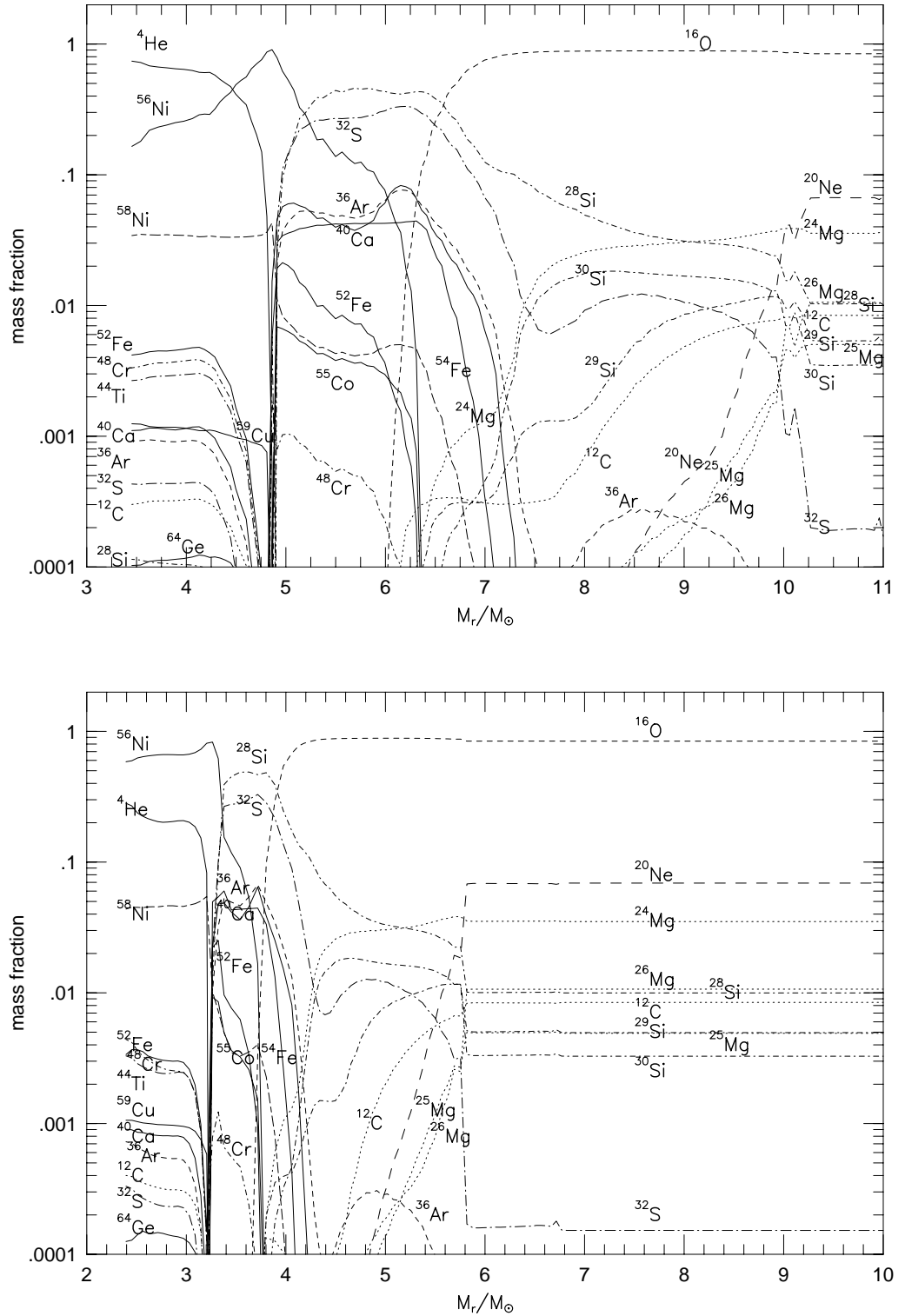


FIG. 2.— Nucleosynthesis in hypernovae and normal core-collapse supernovae for explosion energies of  $E = 100$  (top left),  $30$  (top right),  $10$  (bottom left), and  $1$  (bottom right)  $\times 10^{51}$  ergs. The progenitor model is the  $16M_{\odot}$  He core model.

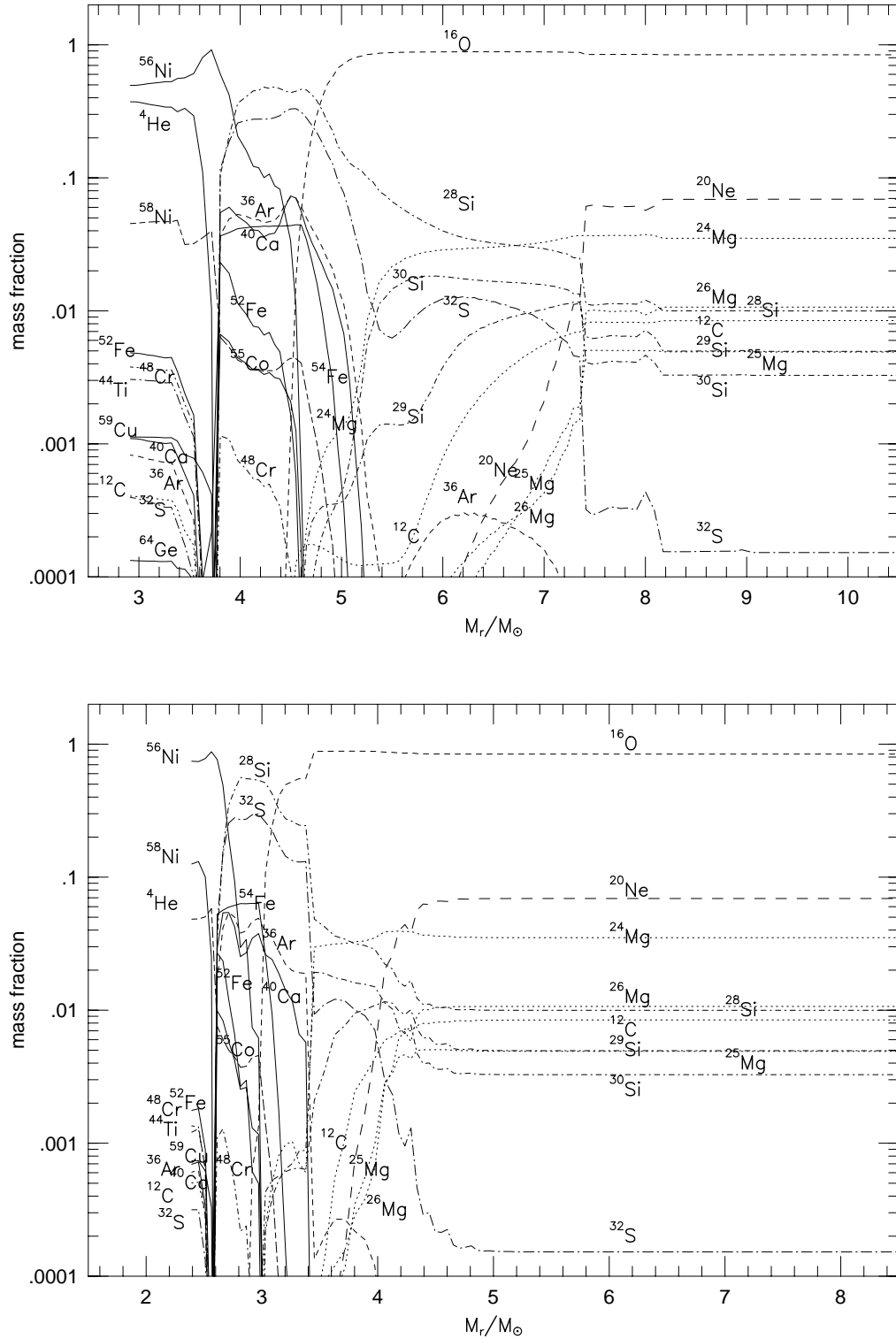


FIG. 2.— Nucleosynthesis in hypernovae and normal core-collapse supernovae for explosion energies of  $E = 100$  (top left),  $30$  (top right),  $10$  (bottom left), and  $1$  (bottom right)  $\times 10^{51}$  ergs. The progenitor model is the  $16M_{\odot}$  He core model.

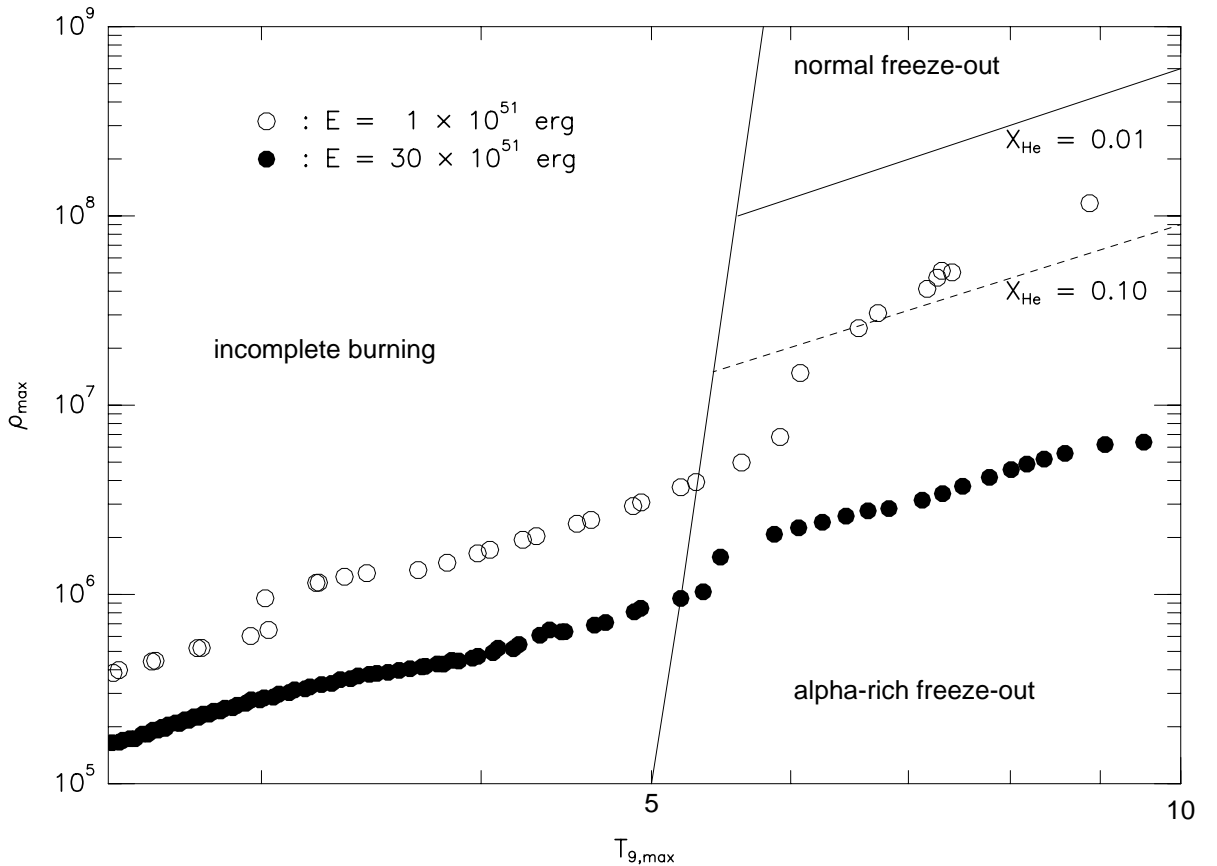


FIG. 3.— The  $\rho$  -  $T$  conditions of individual mass zones at their temperature maximum in hypernovae ( $E = 30 \times 10^{51}$  ergs: filled circles) and normal supernovae ( $E = 1 \times 10^{51}$  erg: open circles). The lines that separate the Si-burning regimes and contour lines for constant  ${}^4\text{He}$  mass fractions are taken from Thielemann et al. (1998).

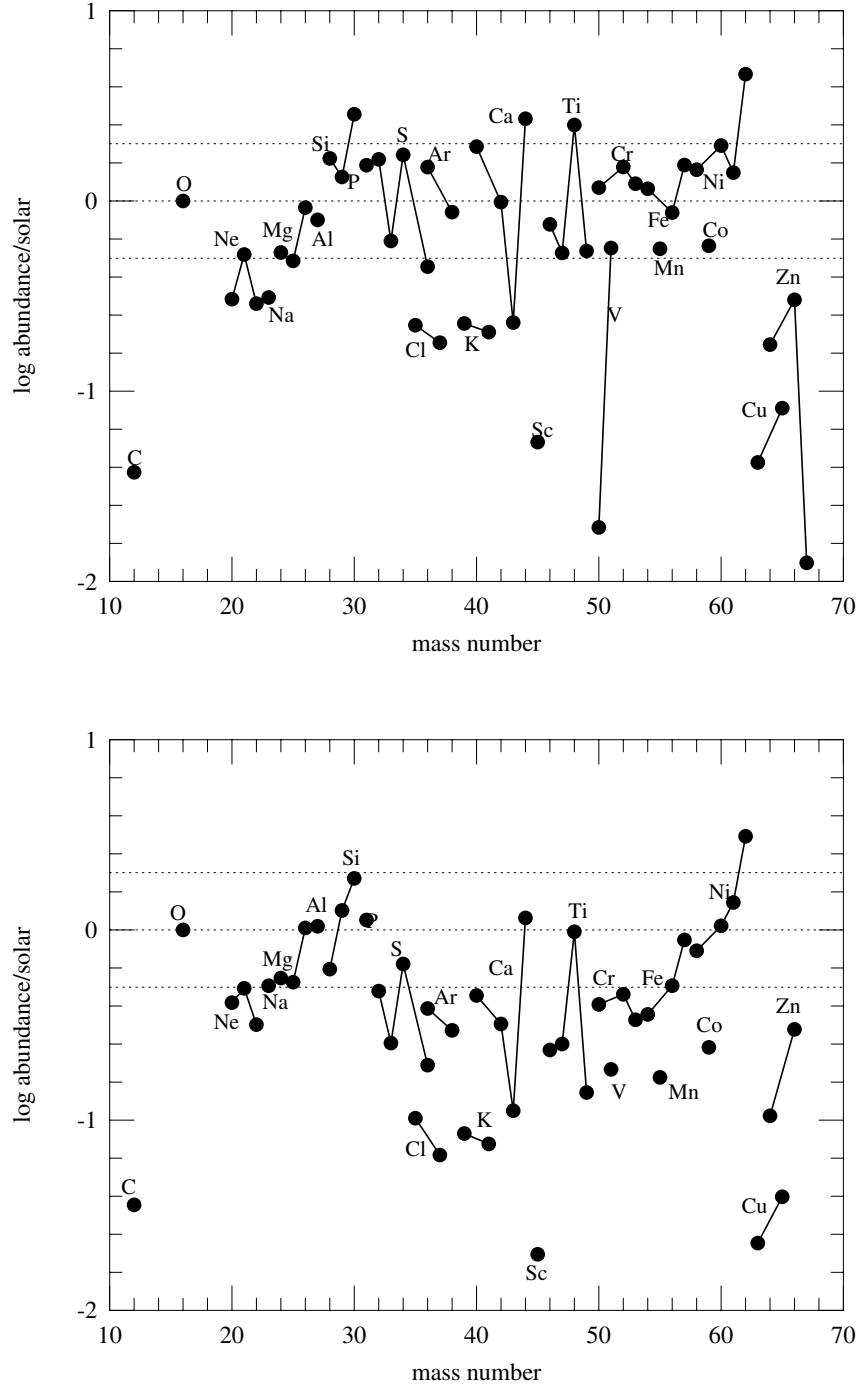


FIG. 4.— Abundances of stable isotopes relative to the solar values for  $E = 100$  (top left),  $30$  (top right),  $10$  (bottom left), and  $1$  (bottom right)  $\times 10^{51}$  ergs. The progenitor model is the  $16M_{\odot}$  He core model (H-rich envelope is not included).

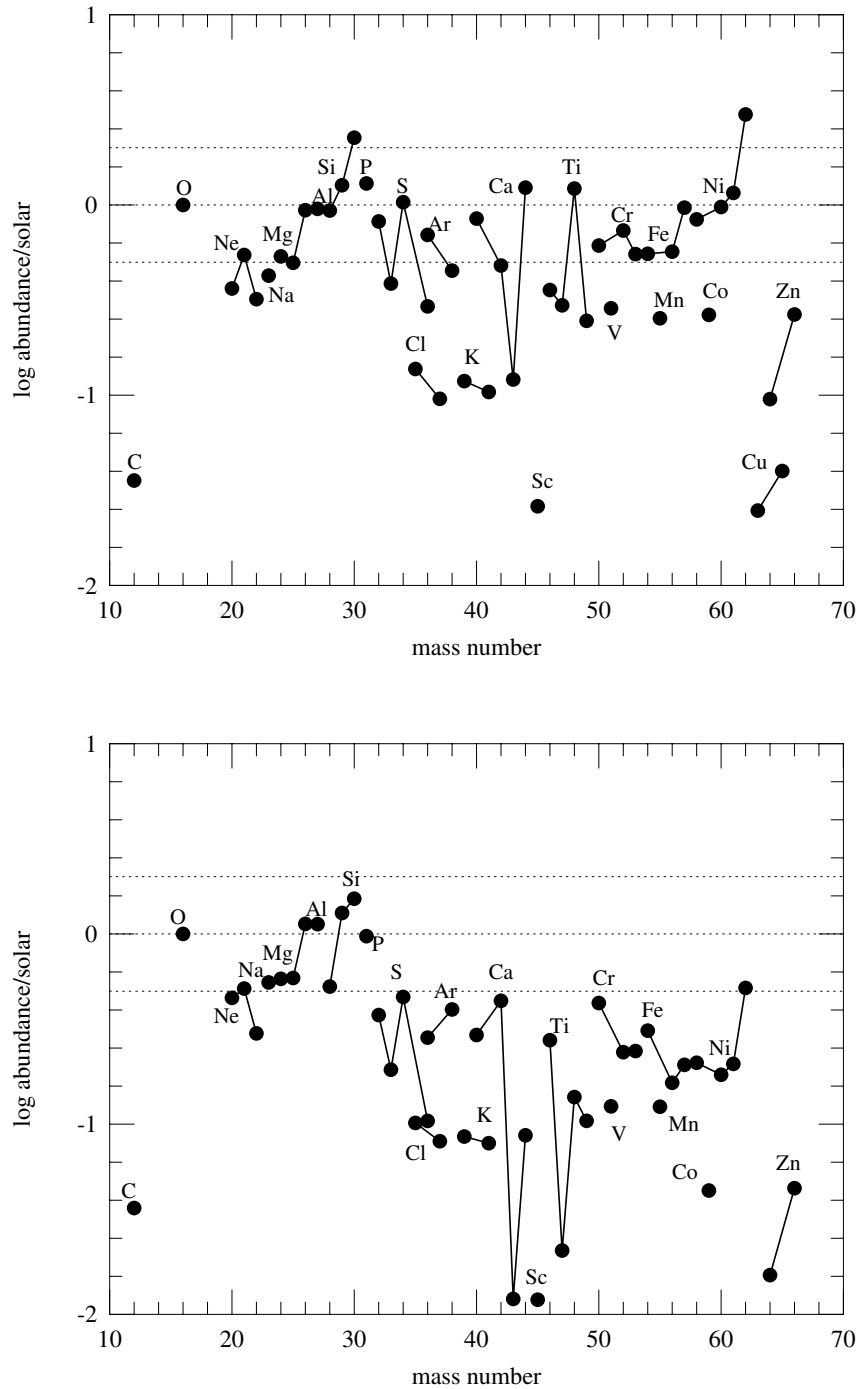


FIG. 4.— Abundances of stable isotopes relative to the solar values for  $E = 100$  (top left),  $30$  (top right),  $10$  (bottom left), and  $1$  (bottom right)  $\times 10^{51}$  ergs. The progenitor model is the  $16M_{\odot}$  He core model (H-rich envelope is not included).

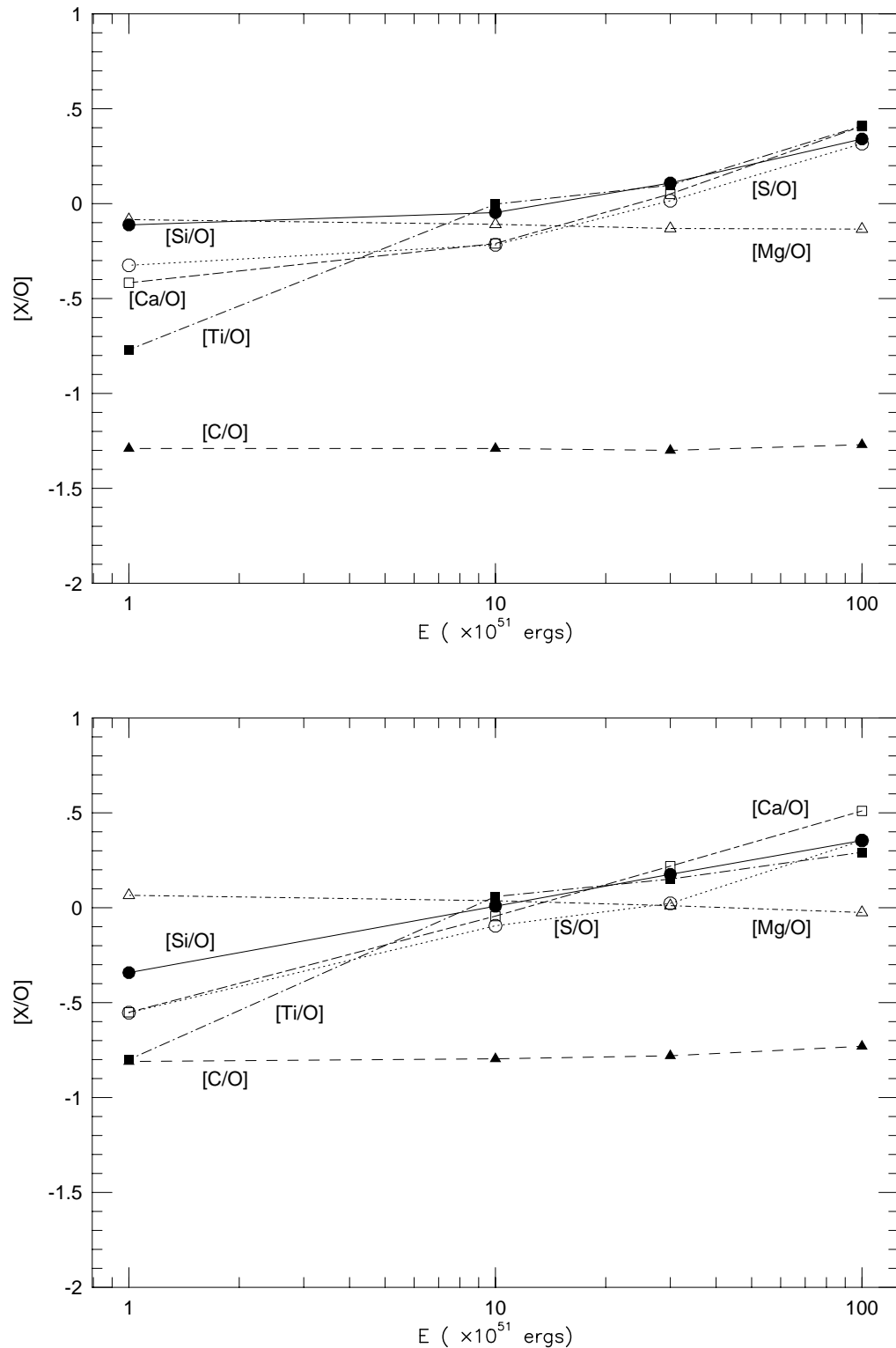


FIG. 5.— Abundance ratios to oxygen relative to solar values as a function of the explosion energy  $E$ . The progenitor model is the  $16M_{\odot}$  He core model (above) and the  $8M_{\odot}$  He core model (below). Products from H-rich envelope are not included in both models.

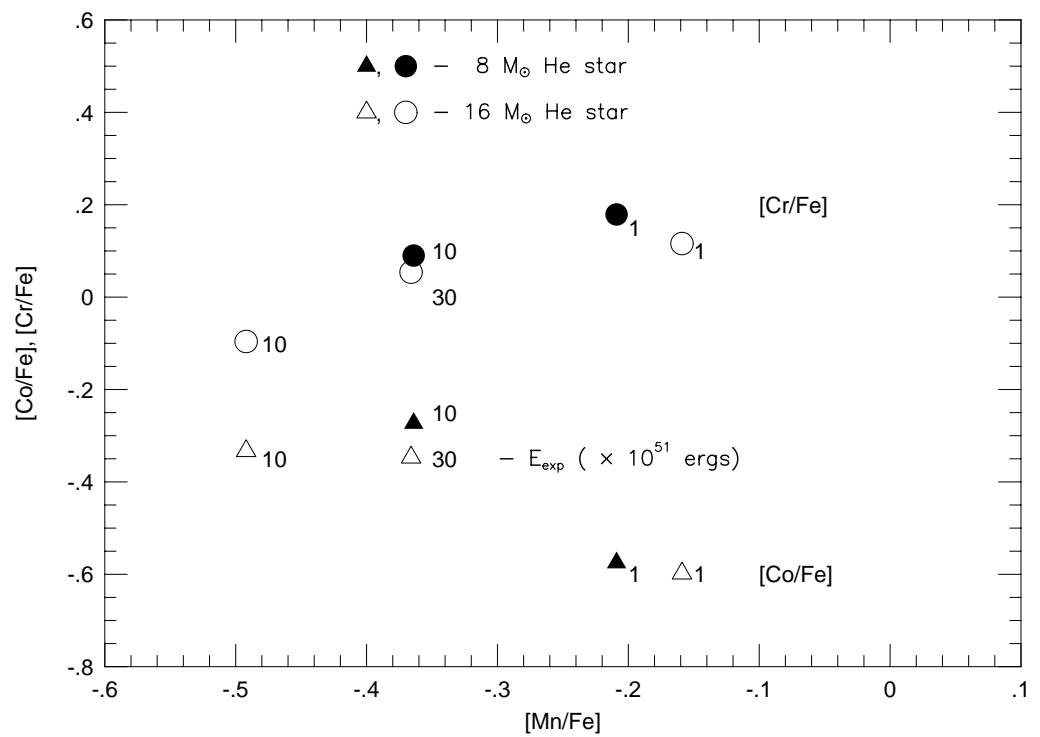


FIG. 6.—  $[\text{Mn/Fe}]$  vs.  $[\text{Co/Fe}]$  and  $[\text{Mn/Fe}]$  for the  $16 M_{\odot}$  He star models with  $E = (1.0 - 30) \times 10^{51}$  ergs, and  $8 M_{\odot}$  He star models with  $E = (1.0 - 10) \times 10^{51}$  ergs.

TABLE 1  
MASS CUTS CHOSEN IN THIS PAPER.

$E$ ( $\times 10^{51}$ ergs) Progenitor	100	30	10	1
$16M_{\odot}$ He core	$3.5M_{\odot}$	$2.9M_{\odot}$	$2.3M_{\odot}$	$2.3M_{\odot}$
$10M_{\odot}$ He core	$2.5M_{\odot}$	$2.5M_{\odot}$	$1.7M_{\odot}$	$1.7M_{\odot}$
$8M_{\odot}$ He core	$2.4M_{\odot}$	$1.9M_{\odot}$	$1.7M_{\odot}$	$1.7M_{\odot}$
$6M_{\odot}$ He core	$2.3M_{\odot}$	$1.8M_{\odot}$	$1.6M_{\odot}$	$1.6M_{\odot}$

TABLE 2

NUCLEOSYNTHESIS PRODUCTS ( $M_{\odot}$ ) OF HYPERNOVAE (AND NORMAL SUPERNOVAE) AFTER DECAY OF RADIOACTIVE SPECIES FOR VARIOUS EXPLOSION ENERGIES. THE PROGENITOR MODEL IS THE  $16M_{\odot}$  HE CORE MODEL.

$E$ ( $\times 10^{51}$ ergs) species	100	30	10	1	$E$ species	100	30	10	1
$^4$ He	2.65	2.20	2.11	1.96	$^{43}$ Ca	1.89E-05	1.25E-05	1.27E-05	1.46E-06
$^{12}$ C	1.05E-01	1.25E-01	1.38E-01	1.49E-01	$^{44}$ Ca	3.24E-03	1.85E-03	1.89E-03	1.53E-04
$^{13}$ C	5.97E-07	2.75E-07	2.35E-07	1.56E-08	$^{46}$ Ca	6.19E-10	5.04E-10	3.18E-10	1.20E-10
$^{14}$ N	1.22E-04	1.22E-04	1.22E-04	1.21E-04	$^{48}$ Ca	7.03E-13	2.17E-13	2.45E-13	2.35E-14
$^{15}$ N	9.23E-08	2.44E-08	1.83E-08	1.01E-08	$^{45}$ Sc	1.59E-06	9.59E-07	7.94E-07	5.14E-07
$^{16}$ O	6.21	7.77	8.49	9.08	$^{46}$ Ti	1.39E-04	8.24E-05	5.90E-05	7.45E-05
$^{17}$ O	2.04E-07	2.30E-07	1.85E-07	8.26E-08	$^{47}$ Ti	9.25E-05	6.44E-05	5.97E-05	5.50E-06
$^{18}$ O	2.37E-07	1.71E-07	1.58E-07	1.63E-07	$^{48}$ Ti	4.51E-03	2.74E-03	2.40E-03	3.65E-04
$^{19}$ F	4.32E-08	4.12E-09	6.08E-10	4.31E-10	$^{49}$ Ti	7.45E-05	4.20E-05	2.61E-05	2.08E-05
$^{20}$ Ne	2.97E-01	4.44E-01	5.53E-01	6.58E-01	$^{50}$ Ti	4.88E-09	2.94E-09	1.76E-09	2.12E-10
$^{21}$ Ne	1.62E-03	2.12E-03	2.09E-03	2.34E-03	$^{50}$ V	1.24E-08	7.26E-09	5.12E-09	3.85E-09
$^{22}$ Ne	3.78E-02	5.23E-02	5.69E-02	5.74E-02	$^{51}$ V	1.54E-04	9.75E-05	6.88E-05	4.94E-05
$^{23}$ Na	9.05E-03	1.55E-02	2.03E-02	2.37E-02	$^{50}$ Cr	6.78E-04	4.41E-04	3.20E-04	3.66E-04
$^{24}$ Mg	2.26E-01	2.83E-01	3.22E-01	3.59E-01	$^{52}$ Cr	1.76E-02	1.07E-02	7.30E-03	4.07E-03
$^{25}$ Mg	2.73E-02	3.51E-02	4.10E-02	4.84E-02	$^{53}$ Cr	1.67E-03	9.34E-04	6.24E-04	4.80E-04
$^{26}$ Mg	5.97E-02	7.60E-02	9.07E-02	1.07E-01	$^{54}$ Cr	3.83E-07	2.28E-07	1.61E-07	1.85E-07
$^{27}$ Al	3.85E-02	5.78E-02	6.92E-02	7.97E-02	$^{55}$ Mn	6.05E-03	3.42E-03	2.48E-03	1.95E-03
$^{28}$ Si	9.11E-01	6.37E-01	4.63E-01	4.21E-01	$^{54}$ Fe	6.92E-02	4.13E-02	2.94E-02	2.71E-02
$^{29}$ Si	3.84E-02	4.57E-02	4.98E-02	5.42E-02	$^{56}$ Fe	8.47E-01	6.93E-01	6.79E-01	2.35E-01
$^{30}$ Si	5.59E-02	5.52E-02	4.99E-02	4.38E-02	$^{57}$ Fe	3.66E-02	2.87E-02	2.87E-02	7.10E-03
$^{31}$ P	6.55E-03	6.90E-03	6.56E-03	6.05E-03	$^{58}$ Fe	1.34E-07	7.62E-08	5.26E-08	5.13E-08
$^{32}$ S	5.30E-01	3.29E-01	2.09E-01	1.76E-01	$^{59}$ Co	1.59E-03	9.05E-04	9.04E-04	1.79E-04
$^{33}$ S	1.63E-03	1.28E-03	9.20E-04	7.48E-04	$^{58}$ Ni	5.78E-02	4.16E-02	4.21E-02	1.22E-02
$^{34}$ S	2.65E-02	1.96E-02	1.37E-02	1.03E-02	$^{60}$ Ni	3.09E-02	1.93E-02	2.27E-02	4.21E-03
$^{36}$ S	2.33E-05	1.89E-05	1.37E-05	7.86E-06	$^{61}$ Ni	1.03E-03	1.06E-03	1.40E-03	2.22E-04
$^{35}$ Cl	5.87E-04	4.54E-04	3.70E-04	3.93E-04	$^{62}$ Ni	1.06E-02	8.56E-03	9.72E-03	1.74E-03
$^{37}$ Cl	1.63E-04	1.08E-04	8.12E-05	1.08E-04	$^{64}$ Ni	1.48E-11	3.50E-12	4.04E-12	6.10E-13
$^{36}$ Ar	1.02E-01	5.90E-02	3.58E-02	2.83E-02	$^{63}$ Cu	2.09E-05	1.53E-05	1.53E-05	1.97E-06
$^{38}$ Ar	1.17E-02	7.56E-03	5.43E-03	7.85E-03	$^{65}$ Cu	1.86E-05	1.14E-05	1.24E-05	1.36E-06
$^{40}$ Ar	3.21E-07	2.71E-07	1.84E-07	9.94E-08	$^{64}$ Zn	1.45E-04	9.87E-05	1.19E-04	1.95E-05
$^{39}$ K	6.08E-04	3.98E-04	3.12E-04	3.37E-04	$^{66}$ Zn	1.47E-04	1.62E-04	2.00E-04	3.28E-05
$^{41}$ K	4.26E-05	2.71E-05	2.14E-05	2.42E-05	$^{67}$ Zn	9.06E-07	6.92E-07	6.15E-07	4.89E-08
$^{40}$ Ca	9.87E-02	5.42E-02	3.16E-02	2.20E-02	$^{68}$ Zn	2.40E-07	1.30E-07	1.15E-07	1.47E-08
$^{42}$ Ca	3.49E-04	2.13E-04	1.55E-04	2.31E-04	$^{70}$ Zn	5.89E-12	2.55E-12	4.60E-12	4.61E-13

TABLE 3

NUCLEOSYNTHESIS PRODUCTS ( $M_{\odot}$ ) OF HYPERNOVAE (AND NORMAL SUPERNOVAE) AFTER DECAY OF RADIOACTIVE SPECIES FOR VARIOUS EXPLOSION ENERGIES. THE PROGENITOR MODEL IS THE  $10M_{\odot}$  HE CORE MODEL.

$E$ ( $\times 10^{51}$ ergs) species	100	30	10	1	$E$ species	100	30	10	1
$^4\text{He}$	3.16	2.45	2.48	2.35	$^{43}\text{Ca}$	2.35E-05	5.02E-06	8.67E-06	2.10E-06
$^{12}\text{C}$	2.01E-01	2.30E-01	2.43E-01	2.55E-01	$^{44}\text{Ca}$	3.16E-03	6.45E-04	1.22E-03	1.81E-04
$^{13}\text{C}$	2.03E-05	8.34E-06	1.66E-06	3.55E-07	$^{46}\text{Ca}$	3.25E-10	2.43E-10	1.99E-10	7.41E-11
$^{14}\text{N}$	6.46E-04	6.38E-04	6.38E-04	6.38E-04	$^{48}\text{Ca}$	3.69E-12	1.04E-13	1.17E-13	1.26E-14
$^{15}\text{N}$	1.61E-07	6.14E-08	3.80E-08	1.87E-08	$^{45}\text{Sc}$	1.00E-06	6.83E-07	9.60E-07	6.71E-07
$^{16}\text{O}$	1.92	2.88	3.46	3.96	$^{46}\text{Ti}$	8.33E-05	6.48E-05	4.31E-05	1.45E-04
$^{17}\text{O}$	9.30E-07	3.78E-07	2.82E-07	1.25E-07	$^{47}\text{Ti}$	1.09E-04	2.21E-05	6.89E-05	1.19E-05
$^{18}\text{O}$	3.49E-05	5.00E-05	6.33E-05	7.73E-05	$^{48}\text{Ti}$	4.27E-03	1.22E-03	1.90E-03	2.92E-04
$^{19}\text{F}$	3.55E-08	4.41E-08	1.11E-08	4.70E-09	$^{49}\text{Ti}$	4.73E-05	3.86E-05	3.08E-05	1.53E-05
$^{20}\text{Ne}$	1.62E-02	1.43E-01	2.82E-01	4.59E-01	$^{50}\text{Ti}$	2.31E-09	1.97E-09	1.22E-09	9.58E-10
$^{21}\text{Ne}$	3.99E-04	6.82E-04	1.31E-03	1.88E-03	$^{50}\text{V}$	6.57E-09	5.29E-09	3.34E-09	1.32E-08
$^{22}\text{Ne}$	3.56E-02	4.99E-02	5.90E-02	6.33E-02	$^{51}\text{V}$	1.36E-04	7.57E-05	8.47E-05	6.21E-05
$^{23}\text{Na}$	1.97E-03	4.65E-03	1.09E-02	1.79E-02	$^{50}\text{Cr}$	4.21E-04	3.81E-04	3.13E-04	7.97E-04
$^{24}\text{Mg}$	6.24E-02	1.23E-01	1.62E-01	2.06E-01	$^{52}\text{Cr}$	1.29E-02	8.50E-03	8.00E-03	2.81E-03
$^{25}\text{Mg}$	4.01E-03	1.18E-02	1.94E-02	2.89E-02	$^{53}\text{Cr}$	1.09E-03	8.89E-04	7.40E-04	5.32E-04
$^{26}\text{Mg}$	2.06E-02	2.88E-02	3.13E-02	4.21E-02	$^{54}\text{Cr}$	2.46E-07	1.95E-07	1.34E-07	9.90E-07
$^{27}\text{Al}$	6.30E-03	1.58E-02	2.48E-02	3.51E-02	$^{55}\text{Mn}$	4.14E-03	3.27E-03	2.90E-03	2.26E-03
$^{28}\text{Si}$	5.66E-01	5.08E-01	4.01E-01	3.34E-01	$^{54}\text{Fe}$	4.36E-02	3.62E-02	3.23E-02	4.32E-02
$^{29}\text{Si}$	1.18E-02	1.55E-02	1.73E-02	1.92E-02	$^{56}\text{Fe}$	7.15E-01	4.66E-01	5.64E-01	2.00E-01
$^{30}\text{Si}$	2.79E-02	2.62E-02	2.44E-02	1.94E-02	$^{57}\text{Fe}$	3.56E-02	1.70E-02	2.93E-02	8.91E-03
$^{31}\text{P}$	3.09E-03	3.37E-03	3.42E-03	3.06E-03	$^{58}\text{Fe}$	8.83E-08	6.36E-08	4.38E-08	2.06E-07
$^{32}\text{S}$	3.35E-01	2.70E-01	2.00E-01	1.32E-01	$^{59}\text{Co}$	1.99E-03	4.38E-04	1.22E-03	3.32E-04
$^{33}\text{S}$	1.22E-03	1.09E-03	8.90E-04	8.44E-04	$^{58}\text{Ni}$	6.07E-02	2.00E-02	9.89E-02	2.99E-02
$^{34}\text{S}$	1.87E-02	1.51E-02	1.14E-02	1.34E-02	$^{60}\text{Ni}$	3.54E-02	1.07E-02	1.58E-02	5.02E-03
$^{36}\text{S}$	4.44E-05	9.08E-06	7.78E-06	5.14E-06	$^{61}\text{Ni}$	9.76E-04	4.50E-04	1.33E-03	3.79E-04
$^{35}\text{Cl}$	7.29E-04	3.81E-04	3.24E-04	4.66E-04	$^{62}\text{Ni}$	1.12E-02	3.41E-03	1.87E-02	5.56E-03
$^{37}\text{Cl}$	1.25E-04	9.04E-05	6.58E-05	1.31E-04	$^{64}\text{Ni}$	4.57E-11	2.68E-12	2.76E-12	4.15E-13
$^{36}\text{Ar}$	6.44E-02	4.84E-02	3.50E-02	1.90E-02	$^{63}\text{Cu}$	2.26E-05	4.57E-06	3.57E-05	6.90E-06
$^{38}\text{Ar}$	6.83E-03	5.86E-03	3.96E-03	1.36E-02	$^{65}\text{Cu}$	2.14E-05	3.65E-06	1.40E-05	2.98E-06
$^{40}\text{Ar}$	2.36E-06	1.26E-07	1.07E-07	6.92E-08	$^{64}\text{Zn}$	1.60E-04	5.27E-05	6.99E-05	2.36E-05
$^{39}\text{K}$	4.10E-04	2.87E-04	2.48E-04	4.94E-04	$^{66}\text{Zn}$	1.48E-04	5.48E-05	3.59E-04	1.21E-04
$^{41}\text{K}$	2.80E-05	2.05E-05	1.85E-05	3.07E-05	$^{67}\text{Zn}$	9.95E-07	1.51E-07	1.56E-06	2.72E-07
$^{40}\text{Ca}$	6.08E-02	4.43E-02	3.20E-02	1.36E-02	$^{68}\text{Zn}$	3.01E-07	4.01E-08	4.61E-07	1.20E-07
$^{42}\text{Ca}$	2.01E-04	1.59E-04	1.10E-04	4.46E-04	$^{70}\text{Zn}$	1.79E-11	2.16E-12	1.17E-12	2.14E-13

TABLE 4

NUCLEOSYNTHESIS PRODUCTS ( $M_{\odot}$ ) OF HYPERNOVAE (AND NORMAL SUPERNOVAE) AFTER DECAY OF RADIOACTIVE SPECIES FOR VARIOUS EXPLOSION ENERGIES. THE PROGENITOR MODEL IS THE  $8M_{\odot}$  HE CORE MODEL.

$E$ ( $\times 10^{51}$ ergs) species	100	30	10	1	$E$ species	100	30	10	1
$^4\text{He}$	2.25	2.21	2.07	1.95	$^{43}\text{Ca}$	2.96E-06	5.30E-06	6.49E-06	7.12E-07
$^{12}\text{C}$	1.19E-01	1.32E-01	1.40E-01	1.49E-01	$^{44}\text{Ca}$	9.82E-04	7.35E-04	6.34E-04	6.70E-05
$^{13}\text{C}$	7.54E-06	5.69E-06	4.06E-06	3.11E-09	$^{46}\text{Ca}$	7.66E-11	6.28E-11	4.47E-11	1.30E-11
$^{14}\text{N}$	9.46E-04	9.46E-04	9.46E-04	9.46E-04	$^{48}\text{Ca}$	9.36E-14	1.52E-13	1.07E-13	4.62E-15
$^{15}\text{N}$	5.73E-07	5.27E-07	4.09E-07	2.74E-09	$^{45}\text{Sc}$	6.50E-07	4.39E-07	2.29E-07	8.38E-08
$^{16}\text{O}$	1.99	2.47	2.74	3.00	$^{46}\text{Ti}$	4.29E-05	2.64E-05	1.64E-05	4.63E-06
$^{17}\text{O}$	2.89E-07	1.29E-07	8.82E-08	2.64E-08	$^{47}\text{Ti}$	1.53E-05	2.32E-05	2.32E-05	2.95E-06
$^{18}\text{O}$	3.97E-03	5.22E-03	5.87E-03	6.69E-03	$^{48}\text{Ti}$	8.67E-04	9.90E-04	8.90E-04	1.31E-04
$^{19}\text{F}$	9.63E-06	9.79E-06	7.27E-06	3.78E-10	$^{49}\text{Ti}$	2.45E-05	2.04E-05	1.20E-05	5.06E-06
$^{20}\text{Ne}$	1.63E-01	3.28E-01	4.52E-01	6.12E-01	$^{50}\text{Ti}$	7.63E-10	6.15E-10	3.71E-10	1.01E-10
$^{21}\text{Ne}$	1.23E-03	2.08E-03	2.67E-03	3.23E-03	$^{50}\text{V}$	3.02E-09	1.92E-09	1.20E-09	3.38E-10
$^{22}\text{Ne}$	2.62E-02	3.19E-02	3.34E-02	3.39E-02	$^{51}\text{V}$	3.82E-05	3.88E-05	3.18E-05	9.31E-06
$^{23}\text{Na}$	5.20E-03	1.02E-02	1.37E-02	1.85E-02	$^{50}\text{Cr}$	1.50E-04	1.25E-04	8.50E-05	3.81E-05
$^{24}\text{Mg}$	1.02E-01	1.34E-01	1.52E-01	1.68E-01	$^{52}\text{Cr}$	4.84E-03	4.47E-03	3.34E-03	1.24E-03
$^{25}\text{Mg}$	1.28E-02	2.26E-02	3.00E-02	4.01E-02	$^{53}\text{Cr}$	5.96E-04	4.64E-04	2.80E-04	1.18E-04
$^{26}\text{Mg}$	1.47E-02	1.79E-02	2.36E-02	3.24E-02	$^{54}\text{Cr}$	8.51E-08	6.49E-08	4.07E-08	1.26E-08
$^{27}\text{Al}$	1.05E-02	1.46E-02	1.71E-02	1.95E-02	$^{55}\text{Mn}$	1.95E-03	1.51E-03	9.73E-04	4.28E-04
$^{28}\text{Si}$	3.12E-01	2.56E-01	1.89E-01	8.91E-02	$^{54}\text{Fe}$	1.67E-02	1.28E-02	8.65E-03	3.65E-03
$^{29}\text{Si}$	8.04E-03	7.93E-03	7.70E-03	6.61E-03	$^{56}\text{Fe}$	2.37E-01	1.69E-01	1.98E-01	6.09E-02
$^{30}\text{Si}$	1.31E-02	1.14E-02	9.33E-03	5.48E-03	$^{57}\text{Fe}$	9.03E-03	6.53E-03	8.99E-03	1.71E-03
$^{31}\text{P}$	1.88E-03	1.66E-03	1.30E-03	6.41E-04	$^{58}\text{Fe}$	3.40E-08	2.50E-08	1.36E-08	4.09E-09
$^{32}\text{S}$	1.86E-01	1.35E-01	9.03E-02	3.47E-02	$^{59}\text{Co}$	9.54E-04	5.04E-04	3.04E-04	4.65E-05
$^{33}\text{S}$	8.19E-04	6.62E-04	4.76E-04	1.78E-04	$^{58}\text{Ni}$	1.92E-02	1.26E-02	7.78E-03	2.26E-03
$^{34}\text{S}$	9.25E-03	7.22E-03	4.97E-03	1.76E-03	$^{60}\text{Ni}$	1.34E-02	9.16E-03	8.11E-03	1.21E-03
$^{36}\text{S}$	2.74E-06	2.15E-06	1.62E-06	5.93E-07	$^{61}\text{Ni}$	1.43E-04	1.99E-04	3.15E-04	7.17E-05
$^{35}\text{Cl}$	2.80E-04	2.35E-04	1.73E-04	6.15E-05	$^{62}\text{Ni}$	1.79E-03	2.13E-03	2.32E-03	4.97E-04
$^{37}\text{Cl}$	6.09E-05	4.45E-05	2.93E-05	1.01E-05	$^{64}\text{Ni}$	4.21E-12	1.33E-10	2.84E-12	1.68E-13
$^{36}\text{Ar}$	3.86E-02	2.60E-02	1.63E-02	5.94E-03	$^{63}\text{Cu}$	1.45E-05	2.10E-05	4.61E-06	7.78E-07
$^{38}\text{Ar}$	3.42E-03	2.29E-03	1.52E-03	4.59E-04	$^{65}\text{Cu}$	1.53E-05	1.51E-05	3.77E-06	6.22E-07
$^{40}\text{Ar}$	4.25E-08	3.47E-08	2.49E-08	8.70E-09	$^{64}\text{Zn}$	3.42E-05	6.28E-05	6.01E-05	8.05E-06
$^{39}\text{K}$	1.77E-04	1.39E-04	9.11E-05	2.60E-05	$^{66}\text{Zn}$	2.39E-05	4.44E-05	3.97E-05	1.20E-05
$^{41}\text{K}$	1.46E-05	1.03E-05	6.21E-06	2.02E-06	$^{67}\text{Zn}$	1.06E-06	3.48E-06	1.57E-07	2.95E-08
$^{40}\text{Ca}$	4.07E-02	2.56E-02	1.53E-02	5.36E-03	$^{68}\text{Zn}$	9.53E-07	5.41E-06	4.26E-08	7.71E-09
$^{42}\text{Ca}$	1.03E-04	6.33E-05	4.01E-05	1.16E-05	$^{70}\text{Zn}$	1.31E-12	1.19E-12	2.51E-12	4.16E-14

TABLE 5

NUCLEOSYNTHESIS PRODUCTS ( $M_{\odot}$ ) OF HYPERNOVAE (AND NORMAL SUPERNOVAE) AFTER DECAY OF RADIOACTIVE SPECIES FOR VARIOUS EXPLOSION ENERGIES. THE PROGENITOR MODEL IS THE  $6M_{\odot}$  HE CORE MODEL.

$E$ ( $\times 10^{51}$ ergs) species	100	30	10	1	$E$ species	100	30	10	1
$^4\text{He}$	2.17E+00	2.26E+00	2.24E+00	2.10E+00	$^{43}\text{Ca}$	7.02E-07	2.95E-06	7.40E-06	1.11E-06
$^{12}\text{C}$	9.95E-02	1.06E-01	1.10E-01	1.14E-01	$^{44}\text{Ca}$	4.18E-05	3.27E-04	7.01E-04	8.81E-05
$^{13}\text{C}$	1.37E-05	6.72E-06	6.46E-06	5.28E-10	$^{46}\text{Ca}$	3.10E-11	2.36E-11	1.61E-11	9.16E-12
$^{14}\text{N}$	2.70E-03	2.71E-03	2.71E-03	2.71E-03	$^{48}\text{Ca}$	1.48E-13	1.42E-13	1.60E-13	1.12E-14
$^{15}\text{N}$	5.23E-06	4.42E-06	3.43E-06	2.53E-10	$^{45}\text{Sc}$	6.26E-07	2.70E-07	2.35E-07	9.38E-08
$^{16}\text{O}$	8.18E-01	1.10E+00	1.27E+00	1.48E+00	$^{46}\text{Ti}$	2.67E-05	1.76E-05	1.14E-05	3.87E-06
$^{17}\text{O}$	9.46E-08	3.96E-08	2.71E-08	5.49E-09	$^{47}\text{Ti}$	2.00E-06	1.38E-05	3.07E-05	6.06E-06
$^{18}\text{O}$	5.68E-03	6.89E-03	7.67E-03	8.68E-03	$^{48}\text{Ti}$	1.56E-04	4.90E-04	9.44E-04	1.55E-04
$^{19}\text{F}$	1.60E-05	1.16E-05	8.99E-06	3.38E-11	$^{49}\text{Ti}$	1.47E-05	1.25E-05	8.82E-06	3.83E-06
$^{20}\text{Ne}$	3.69E-02	9.64E-02	1.45E-01	2.19E-01	$^{50}\text{Ti}$	3.66E-10	3.41E-10	2.34E-10	8.29E-11
$^{21}\text{Ne}$	6.85E-04	6.72E-04	5.98E-04	2.92E-04	$^{50}\text{V}$	1.70E-09	1.10E-09	7.49E-10	2.65E-10
$^{22}\text{Ne}$	2.33E-02	2.71E-02	2.89E-02	2.93E-02	$^{51}\text{V}$	1.53E-05	2.24E-05	3.51E-05	1.04E-05
$^{23}\text{Na}$	1.28E-03	1.41E-03	1.35E-03	1.10E-03	$^{50}\text{Cr}$	7.94E-05	6.92E-05	6.30E-05	3.39E-05
$^{24}\text{Mg}$	6.21E-02	9.60E-02	1.19E-01	1.48E-01	$^{52}\text{Cr}$	2.17E-03	2.36E-03	2.33E-03	9.43E-04
$^{25}\text{Mg}$	3.99E-03	8.45E-03	1.20E-02	1.78E-02	$^{53}\text{Cr}$	3.49E-04	2.78E-04	1.65E-04	8.44E-05
$^{26}\text{Mg}$	6.60E-03	9.09E-03	1.09E-02	1.65E-02	$^{54}\text{Cr}$	5.04E-08	4.33E-08	2.99E-08	1.19E-08
$^{27}\text{Al}$	5.67E-03	9.43E-03	1.21E-02	1.54E-02	$^{55}\text{Mn}$	1.18E-03	9.47E-04	5.87E-04	3.06E-04
$^{28}\text{Si}$	1.61E-01	1.56E-01	1.34E-01	8.94E-02	$^{54}\text{Fe}$	8.93E-03	7.64E-03	5.78E-03	3.01E-03
$^{29}\text{Si}$	5.84E-03	6.64E-03	8.05E-03	9.79E-03	$^{56}\text{Fe}$	1.35E-01	1.03E-01	1.48E-01	7.22E-02
$^{30}\text{Si}$	1.06E-02	9.05E-03	8.76E-03	7.72E-03	$^{57}\text{Fe}$	5.45E-03	4.19E-03	7.80E-03	3.31E-03
$^{31}\text{P}$	1.22E-03	1.24E-03	1.25E-03	1.15E-03	$^{58}\text{Fe}$	2.72E-08	1.62E-08	1.08E-08	3.88E-09
$^{32}\text{S}$	9.60E-02	7.65E-02	5.73E-02	2.80E-02	$^{59}\text{Co}$	6.57E-04	4.62E-04	4.14E-04	1.28E-04
$^{33}\text{S}$	4.30E-04	3.55E-04	2.87E-04	1.57E-04	$^{58}\text{Ni}$	8.37E-03	1.03E-02	9.84E-03	8.98E-03
$^{34}\text{S}$	4.56E-03	3.84E-03	2.85E-03	1.44E-03	$^{60}\text{Ni}$	9.67E-03	6.37E-03	7.85E-03	2.34E-03
$^{36}\text{S}$	7.28E-06	1.30E-06	9.88E-07	5.56E-07	$^{61}\text{Ni}$	5.32E-05	1.00E-04	2.73E-04	1.74E-04
$^{35}\text{Cl}$	1.65E-04	1.20E-04	1.09E-04	5.99E-05	$^{62}\text{Ni}$	4.27E-04	1.31E-03	2.44E-03	2.27E-03
$^{37}\text{Cl}$	3.39E-05	2.43E-05	1.87E-05	8.30E-06	$^{64}\text{Ni}$	1.75E-09	3.93E-11	2.45E-12	2.43E-13
$^{36}\text{Ar}$	2.21E-02	1.54E-02	1.06E-02	4.70E-03	$^{63}\text{Cu}$	6.61E-06	1.10E-05	1.22E-05	4.92E-06
$^{38}\text{Ar}$	1.60E-03	1.34E-03	9.07E-04	3.67E-04	$^{65}\text{Cu}$	1.78E-06	8.56E-06	5.36E-06	1.72E-06
$^{40}\text{Ar}$	1.15E-07	1.57E-08	1.23E-08	6.28E-09	$^{64}\text{Zn}$	8.62E-05	3.23E-05	1.60E-04	1.51E-05
$^{39}\text{K}$	9.83E-05	7.63E-05	7.10E-05	2.49E-05	$^{66}\text{Zn}$	1.78E-06	1.78E-05	4.35E-05	5.85E-05
$^{41}\text{K}$	8.63E-06	5.76E-06	4.68E-06	1.80E-06	$^{67}\text{Zn}$	1.06E-07	9.58E-07	3.10E-07	2.40E-07
$^{40}\text{Ca}$	2.48E-02	1.63E-02	9.70E-03	4.15E-03	$^{68}\text{Zn}$	1.82E-06	1.27E-06	9.38E-08	1.33E-07
$^{42}\text{Ca}$	5.68E-05	3.94E-05	2.58E-05	9.59E-06	$^{70}\text{Zn}$	2.20E-13	1.56E-12	2.19E-12	1.71E-13

TABLE 6: Nucleosynthesis products ( $M_{\odot}$ ) of Hypernovae (and Normal supernovae) before the onset of Radioactive Decays for various explosion energies. The progenitor model is the  $16M_{\odot}$  He core model.

TABLE 7: Nucleosynthesis products ( $M_{\odot}$ ) of Hypernovae (and Normal supernovae) before the onset of Radioactive Decays for various explosion energies. The progenitor model is the  $10M_{\odot}$  He core model.

TABLE 8: Nucleosynthesis products ( $M_{\odot}$ ) of Hypernovae (and Normal supernovae) before the onset of Radioactive Decays for various explosion energies. The progenitor model is the  $8M_{\odot}$  He core model.

TABLE 9: Nucleosynthesis products ( $M_{\odot}$ ) of Hypernovae (and Normal supernovae) before the onset of Radioactive Decays for various explosion energies. The progenitor model is the  $6M_{\odot}$  He core model.

Tables 6 - 9 are available at

<http://www.astron.s.u-tokyo.ac.jp/~nakamura/research/papers/nakamuratab.ps.gz>

TABLE 10

MAJOR RADIOACTIVE ELEMENTS ( $M_{\odot}$ ) OF HYPERNOVAE (AND NORMAL SUPERNOVAE) FOR VARIOUS EXPLOSION ENERGIES.

Progenitor mass( $M_{\odot}$ )	$E$ ( $\times 10^{51}$ ergs) species	100	30	10	1
16	$^{26}\text{Al}$	3.57E-05	4.50E-05	4.39E-05	5.27E-05
	$^{41}\text{Ca}$	4.25E-05	2.70E-05	2.13E-05	2.42E-05
	$^{44}\text{Ti}$	3.24E-03	1.85E-03	1.89E-03	1.53E-04
	$^{56}\text{Ni}$	8.45E-01	6.92E-01	6.78E-01	2.35E-01
	$^{57}\text{Ni}$	3.65E-02	2.86E-02	2.87E-02	7.06E-03
10	$^{26}\text{Al}$	6.81E-06	2.17E-05	1.89E-05	1.66E-05
	$^{41}\text{Ca}$	2.75E-05	2.04E-05	1.84E-05	3.07E-05
	$^{44}\text{Ti}$	3.16E-03	6.45E-04	1.22E-03	1.81E-04
	$^{56}\text{Ni}$	7.14E-01	4.65E-01	5.63E-01	1.97E-01
	$^{57}\text{Ni}$	3.55E-02	1.70E-02	2.93E-02	8.84E-03
8	$^{26}\text{Al}$	2.08E-03	5.56E-03	8.34E-03	1.23E-02
	$^{41}\text{Ca}$	1.45E-05	1.03E-05	6.19E-06	2.02E-06
	$^{44}\text{Ti}$	9.82E-04	7.35E-04	6.34E-04	6.69E-05
	$^{56}\text{Ni}$	2.37E-01	1.68E-01	1.98E-01	6.09E-02
	$^{57}\text{Ni}$	9.02E-03	6.52E-03	8.98E-03	1.70E-03
6	$^{26}\text{Al}$	5.33E-04	2.42E-03	4.08E-03	6.73E-03
	$^{41}\text{Ca}$	8.60E-06	5.75E-06	4.67E-06	1.80E-06
	$^{44}\text{Ti}$	4.18E-05	3.27E-04	7.01E-04	8.81E-05
	$^{56}\text{Ni}$	1.35E-01	1.03E-01	1.48E-01	7.22E-02
	$^{57}\text{Ni}$	5.44E-03	4.18E-03	7.79E-03	3.30E-03

TABLE 11

ABUNDANCE RATIOS OF IRON-PEAK ELEMENTS FOR VARIOUS EXPLOSION ENERGIES.

Progenitor mass( $M_{\odot}$ )	$E$ ( $\times 10^{51}$ ergs) ratios	100	30	10	1
16	[Cr/Fe]	0.191	0.054	-0.096	0.116
	[Mn/Fe]	-0.273	-0.366	-0.492	-0.159
	[Co/Fe]	-0.066	-0.347	-0.333	-0.598
	[Ni/Fe]	0.313	0.206	0.253	0.073
10	[Cr/Fe]	0.114	0.130	0.160	0.072
	[Mn/Fe]	-0.302	-0.219	-0.353	-0.066
	[Co/Fe]	-0.022	-0.495	-0.130	-0.301
	[Ni/Fe]	0.374	0.064	0.573	0.450
8	[Cr/Fe]	0.183	0.286	0.090	0.179
	[Mn/Fe]	-0.148	-0.114	-0.364	-0.209
	[Co/Fe]	0.138	0.007	-0.273	-0.575
	[Ni/Fe]	0.357	0.348	0.173	0.025
6	[Cr/Fe]	0.221	0.228	0.546	-0.014
	[Mn/Fe]	-0.123	-0.102	-0.459	-0.427
	[Co/Fe]	0.221	0.184	-0.013	-0.210
	[Ni/Fe]	0.332	0.437	0.340	0.484